博士論文

2015年度

Role of 100S ribosomes in protein turnover

（タンパク質のターンオーバーにおける１００Sリボソームの役割）

京都産業大学大学院

工学研究科　生物工学専攻

博士後期課程３年

学生証番号　155243

Shcherbakova Ksenia

Summary

Protein turnover is a balance between protein degradation and synthesis. It has been shown to exist in a growing bacterial cell, and is thus speculated to exist in the stationary phase and the following decay period. In stationary phase, when nutrients become deficient, the amino acids supplied by protein turnover could be critical for survival. Among the potential amino acid sources to support protein turnover, in *E.coli*, ribosomes are the largest. Therefore, their involvement in protein turnover could be essential for maintaining viability. In stationary phase, 70S ribosomes are dimerized to form translationally inactive 100S ribosomes. Three factors regulate 100S formation: RMF and HPF are required to make a dimer, and YfiA is required to dissociate it. The relationship among 100S formation and protein turnover, and even the existence of protein turnover in stationary phase and later, are not well studied. This study focuses on the role of ribosomes and particularly 100S ribosomes in protein turnover in stationary phase and decay period.

In this study, ribosomal proteins S10 and S2 were each fused with GFP to track the fates of these proteins in the stationary growth phase and the following decay period in *E.coli*. Disruptants of the 3 100S-reated genes *(*Δ*rmf,* Δ*hpf*, and Δ*yfiA*) were also prepared in the background of S10-GFP. The fused proteins localized mainly in the cytoplasm, and their amounts were proportional to the amount of viable bacteria.

Both the three S10-GFP strains that lacked genes responsible for regulating 100S ribosomes and S2-GFP strain that was unable to form 100S showed shortened stationary phases. This result indicates that these strains exhibit earlier death in the absence of 100S formation (S2-GFP, S10-GFPΔ*rmf*, and S10-GFPΔ*hpf*) and breakdown (S10-GFPΔ*yfiA*). Therefore, in addition to the mere presence of 100S, the correct timing of 100S formation and breakdown is required to maintain viability. Whether or not 20 amino acids were effective to maintain viability was measured by supplying 20 amino acids at several time points. I here propose a model in which 100S acts as a tentative repository of ribosomes that are protected from degradation and provide a source of amino acids in later growth period.

A new GFP that had been invented by my colleagues, B-maggio, was used in this study. Its brightness and especially the 100-fold resistance against photobleaching enabled semi-quantitative analysis for the first time by fusing *gfp* gene with chromosomal genes.

Table of contents:

Introduction

The degradation of proteins is essential to maintain protein homeostasis, and it leads to the generation of amino acids to synthesize new proteins. This recycling is called protein turnover. It has been shown to exist in a growing bacterial cell, and is thus speculated to exist in the stationary phase and the following decay period. In the growing phase, significant supply of nutrients is accompanied by a balanced consumption, and protein turnover occurs at a low rate in a growing bacterial cell (Koch and Levy, 1955). When nutrients become deficient, the amino acids supplied by protein turnover could become critical for survival. In a bacterial culture, such starvation takes place in a long-time culture with decaying CFU (colony forming unit). After this decay period, the death rate is reduced by its adaptation mechanisms involving GASP mutations (Finkel, 2006; Zambrano et al., 1993).

In terms of protein turnover in *E. coli*, ribosomes are the largest amino acid source among proteins or proteinous particles, and ribosomes occupy up to 28% of the dry mass (Bremer and Dennis, 1996). In the growing phase, ribosome per culture volume is exponentially increasing according to growth. In the transition period from exponential phase to stationary phase, its increase slows down and usually reaches a plateau in stationary phase. The ribosome synthesis is determined by the amount of available rRNAs, and excess ribosomal proteins are degraded (Keener and Nomura, 1996). During stationary phase, the level of ribosomes is maintained approximately constant (Piir et al., 2011), although rRNA cleavage as quality control is maintained (Basturea et al., 2011). After stationary phase, a rapid decay of CFU due to starvation takes place. For *E. coli* cultured in LB medium at 37°C it happens after one day in a liquid culture.

In *E. coli*, the translating 70S ribosome is resistant to degradation, and free 30S and 50S subunits are the best substrates for degradation triggered by carbon starvation (Zundel et al., 2009). Consistently, starvation of various nutrients (Ben-Hamida and Schlessinger, 1966) and Mg^{2+} ion (McCarthy, 1962) are known to induce ribosome degradation. Therefore, the degradation during the decay period could be a key step in protein turnover in relation to viability. In the degradation induced by phosphate depletion, a decrease of two thirds of the acid-insoluble RNA was observed at the

middle time point of the decay period (Davis et al., 1986). However, the correlation with the protein turnover is not yet clear.

In addition to degradation, a universal form of inactivation of proteins is inclusion bodies, which were originally defined as loose aggregates of overproduced proteins with their secondary structures retained but their tertiary structures disturbed (Kane and Hartley, 1988; Kopito, 2000; Needham and Mastaglia, 2007; Rajan et al., 2001). However, the inactivation of the proteins in inclusion bodies is usually moderate, and thus both enzymatic activity of enzymes and fluorescence of fluorescent proteins can be preserved (García-Fruítos et al., 2005). Inclusion bodies exist even in exponentially growing *E. coli* cells, and many ribosomal proteins in aberrant form are included, suggesting the role of inclusion bodies as a temporary trash organelle (Maisonneuve et al., 2008). Whether or not bacteria *in vivo* can use their own proteins accumulated as inclusion bodies as a source of amino acids is an interesting question in terms of protein turnover, that hasn't been studied.

The bacterial ribosome has a specific translationally inactive form called 100S ribosome (Wada et al., 1990), which is essentially a dimeric 70S ribosome (Fig.1). In *E. coli*, transcription of *rmf* is activated by (p)ppGpp, a global regulator responding to amino acid starvation and other types of stress (Izutsu et al., 2001). RMF dimerizes 70S to 90S in the following two-step reaction:

$$\text{two } 70S \rightarrow 90S \rightarrow 100S \qquad (1)$$

Two more factors with 40% sequence homology with each other, HPF and YfiA (also knows as RaiA and Protein Y), make or dissociate 100S, respectively (Maki et al., 2000; Ueta et al., 2005). HPF binds to 100S exclusively, while YfiA is mostly found on 70S particles, but in the early stationary phase a small amount of it was also found in 100S fraction (Maki et al., 2000), which may indicate a transitory period of YfiA and HPF competition before the equilibrium of 100S and YfiA-bound 70S is established. However, it is not yet completely understood, whether YfiA acts as association inhibitor, or as dissociation enhancer, or both. YfiA and HPF bind to ribosomes more tightly than RMF: *in vitro* they cannot be washed off by high-salt buffer, while RMF completely dissociates from the ribosome with this treatment (Maki et al., 2000). The existence of 100S is likely to be universal in bacteria, but its mechanism of formation, and probably its biological significance, are not universal (Yoshida and Wada, 2014). The transient

formation of 100S and RMF seem to be conserved only in enterobacteria, and RMF also was found in some other gamma-proteobacteria, while the majority of bacteria have no RMF. In bacteria that don't have RMF, 100S is formed with the help of just one factor, long HPF, which is highly conserved (Ueta et al., 2008). Phylogenetic analysis suggests that the long HPF is an ancestor of its other homologs, short HPF and YfiA. After the short HPF diverged from the long HPF in proteobacteria, they lost 100S, and later gamma proteobacteria acquired RMF that allowed them to form 100S (Ueta et al., 2005; 2013).

The relationship among ribosome degradation, inclusion body formation, 100S formation, and cell death has to be studied to understand the protein turnover in the decay period. In *E. coli,* 100S is known to dissociate as soon as a fresh medium has been added (Aiso et al., 2005), and it was therefore called the hibernation form of ribosome (Yoshida et al., 2002). However, its role in the late stationary phase is still unclear. In the literature, the level of ribosomes has been generally quantitated as the amount of rRNA (Piir et al., 2011), whereas in the study of protein turnover, ribosomal proteins must be quantitated. Therefore, we constructed S10-GFP fusion protein by inserting *gfp* downstream of the essential chromosomal *rpsJ* gene (encoding ribosomal protein S10) to follow its fate. By developing a new form of GFP, we solved several problems in using GFP fluorescence quantitatively. We also constructed another GFP protein fusion with the essential *rpsB* gene (encoding ribosomal protein S2) as a negative control strain for 100S formation. Due to the bulky GFP moiety, the S2-GFP strain cannot form 100S, as the intact S2-S2 contact surface is required for 100S formation (Kato et al., 2010). We also prepared deletion mutants (*Δrmf, Δhpf, and ΔyfiA*) with the S10-GFP background.

The comparison among the amounts of cytoplasmic and insoluble S10-GFP, the level of 100S, and the CFU in stationary phase and the decay period showed that most S10-GFP protein stays in cytoplasm and its amount is temporally proportional to CFU. Comparison with other mutant strains revealed that not only the mutants unable to form 100S, but also the mutant unable to dissociate 100S, die earlier and degrade their ribosomes earlier than the parental S10-GFP strain, implying that both the formation and the dissociation of 100S must be punctual for the maintenance of viability. Therefore, an additional function of 100S is likely to temporarily protect the ribosomes

from degradation and to supply amino acids by degradation for new translation at an appropriate time. We propose a model that 100S is a repository of ribosomes protected from degradation, which provides the cell with amino acids later when necessary.

Results

Growth and appearance of constructed strains

We first labeled a ribosomal protein with GFP. We developed a new form of GFP, B-maggio (PCT/JP2014/081308), which is suitable for a quantitative use, as described below. To remove interference of the wild-type allele, we fused *gfp* gene to the chromosomal *rpsJ* gene in W3110 strain, resulting in strain HN3611, referred to as S10-GFP hereafter. *RpsJ* is the first gene of an operon consisting of essential genes (Fig.2A), therefore a big insertion could disrupt its regulation and affect the growth. To avoid this the antibiotic resistance cassette was removed, which resulted in a very small insertion downstream to the *rpsJ-gfp* (Fig.2B). We also prepared three disruptants of 100S-related genes, Δ*rmf*, Δ*hpf*, and Δ*yfiA* in the background of S10-GFP. In addition, we fused GFP with the essential S2 as a negative control that is incapable of forming 100S. Structural analysis of 100S has previously implicated the S2-S2 contact in its formation (Kato *et al.*, 2010). This contact is likely to be hampered by the fusion of S2 with the bulky GFP.

The growth curves in the pre-synchronized culture are plotted in Figs. 3A and 3B. Although there are time lags for the three disruptants, 4 h for Δ*rmf* and Δ*hpf*, and 1 h for Δ*yfiA*, the observed growth rates in exponential phase were all similar. Especially, S10-GFPΔ*rmf* and S10-GFPΔ*hpf,* which are both lacking a protein required for the formation of 100S*,* showed essentially the same growth curve, including the lag. In addition, the saturation levels of OD_{600} were also similar (OD_{600}= 6) for the five strains as well as W3110, showing that the fusions to GFP and the additional mutations do not disturb their optimal growth.

The microscopic examination of S10-GFP showed distinct temporal changes of images of cells. In exponential phase, the observed fluorescence is localized between the inner membrane and the nucleoid, consistently with the expected localization of ribosomes. In stationary phase, typically at 6 h for S10-GFP, fluorescence spreads to encompass the entire cytoplasm and becomes more homogeneous (Fig.3C). At later hours, spots of relatively higher fluorescence start appearing mostly near cell poles. Fluorescence intensity of the homogeneous background then gradually decreases, while the intensity of the foci increases (Fig.3D). Appearance of these foci suggests that inclusion bodies are formed in decay period, which is demonstrated in a later section.

Time course of 100S formation

Since 100S formation is sensitive to the medium and conditions, we directly ultracentrifuged the cell lysates of the 5 strains cultured under our conditions (Figs. 4A-E) as well as a marker strain with 50S labeled with a red form of GFP and S10 labeled with a green GFP (Fig. 4F). As expected, 100S appears only for S10-GFP and S10-GFPΔ*yfiA*. We plotted the ratio of 100S to the amount of combined 70S and 100S combined as a function of time (Fig. 4G). In S10-GFP, 100S starts forming at 6 h and almost disappears by 18 h with a peak at around 9-12 h, whereas the stationary phase lasts until at least 24 h in S10-GFP, as shown below (Fig. 12). Therefore, the level of 100S is a marker of only a part of stationary state rather than the whole stationary state.

The strain S10-GFPΔ*yfiA* showed the same level of 100S at 9h as S10-GFP strain, but a more persistent accumulation up to 18 h (Fig. 4E), consistently with the role of YfiA in dissociation of 100S (Ueta *et al.*, 2005). Δ*yfiA* mutant has also been previously shown to have a more persistent 100S formation compared to the parental W3110 strain (Ueta *et al.*, 2005). 90S was not observed in S10-GFPΔ*hfp* in our experiment (Fig. 4D), which is in agreement with the previous report that 90S is observable only in the double disruptant Δ*hfp*Δ*yfiA* (Ueta *et al.*, 2005). The absence of 90S in the Δ*hfp* strain may be due to an artifact *in vitro* because ribosome concentration in vitro is orders of magnitude less than *in vivo*, shifting the binding equilibrium towards dissociation in the presence of YfiA (Ueta et al., 2008).

Quantitation of ribosomes with S10-GFP

There are three difficulties in using GFP for quantitation of its fused protein. The first is the maturation of the fluorophore, 4-(p-Hydroxybenzylidene)-5-imidazolinone (Shimomura, 1979), which is formed in two steps: the correct folding of the nascent polypeptide and the oxidative formation of the fluorophore (Fig.5, for details see Stepanenko *et al.*, 2011). Therefore, fluorescent and non-fluorescent GFP molecules always coexist both *in vivo* and *in vitro*. The fraction of the fluorescent molecules, which is usually significantly lower than 1, depends on the time after translation, on the *gfp* allele, and on the protein fused to the GFP as well as the redox atmosphere in cells. These effects are difficult to be determined, hindering quantitation of the fused protein, which becomes unreliable during the growing phase and early stationary phase before

maturation of GFP has been completed. Only after enough time for maturation is allowed following translation, and physiological atmosphere becomes stable, the total fluorescence becomes proportional to the amount of the GFP *in vivo*. Fortunately, in our case, this situation seems to take place in the S10-GFP culture after 6 h, as described below.

The second difficulty takes place when GFP moiety of a fusion protein has different susceptibility to proteolysis from the rest of the protein. To avoid this difficulty, the size of the GFP-containing polypeptide must be monitored with SDS polyacrylamide gel electrophoresis with the reducing reagent omitted to maintain fluorescence.

The third difficulty is photobleaching. Generally, GFP is more resistant to photobleaching than organic dyes due to the ß-can structure that protects the fluorophore from the reactive oxygen species in the solvent. Still, the bleaching affects measurements. This problem was addressed by developing a bright but photostable form of GFP, B-maggio. It is as bright as Venus (Nagai *et al.*, 2002) and GFPuv4 (Ito *et al.*, 1999), which has been so far the brightest in *E. coli* and bright enough expressed from chromosome without over-expression from plasmids (Fig. 3C). The most important characteristic for B-maggio is its stability. It is 100-fold or more resistant to photobleaching *in vivo* and *in vitro* than Venus and GFPuv4. When the measurement of fluorescence intensity of S10-GFP was done under conditions optimized for this study (see Experimental Procedures), the measured value didn't show any decrease (due to photobleaching) even after 5 min of continuous irradiation with excitation light (Table I-1,2).

Novel fluorescent proteins with enhanced properties are developed by substituting various amino acids, which alters folding of the protein and adds/removes reactive functionalities, in a process. It is commonly achieved by subjecting bacteria bearing a gene of a certain fluorescent protein to many rounds of directed evolution, where clones with desired changes in the properties of the fluorescent protein are selected. Another approach is the rational design of proteins by trying to adapt mutations that are known to have enhanced properties of other proteins. The substitutions in B-Maggio are listed in the Table II, together with those in Venus, FPuv4, and mCherry. The exact mechanism of photobleaching in fluorescent proteins is

essentially unknown, but some proposed mechanisms include the cis-trans isomerization of the fluorophore, and decarboxylation of glutamic acid in the vicinity of the fluorophore, resulting in a different hydrogen-bonding network (Auerbach et al., 2014; Shaner et al., 2008; Habuchi et al., 2004). Therefore, subtle changes in conformation of the fluorescent protein in the vicinity of the fluorophore may either reduce the space needed for the cis-trans isomerization, or reduce the possible intramolecular electron transfer from reactive groups, such as glutamic acid, located in the fluorophore pocket (Adam et al., 2009).

When the crude extracts of S10-GFP strain cultured for 12 h were analyzed, the fluorescence intensity of S10-GFP protein in agarose gel was the same as in polyacrylamide gel (Table III-1). The fluorescent stability of the GFP against SDS depends on the fused polypeptide, but fortunately, the S10-GFP protein is stable under the conditions employed. In the presence of 15% glycerol, its fluorescence was unchanged in the presence and absence of SDS (Table III-2, 3), enabling us to extract S10-GFP protein from the cell aggregates by solubilizing the insoluble proteins with SDS. Because of these stabilities of S10-GFP protein, the fluorescence intensities of electrophoretic bands can be quantitatively compared.

To confirm the maturation of the fluorophore as fluorescence intensity per amount of S10-GFP polypeptide, we stained the gel with Coomassie Brilliant Blue. Our cytosolic fraction is a crude lysate containing all soluble proteins, and thus S10-GFP cannot be distinguished as a single band among the other bands. We thus searched for a seemingly isolated single band representing ribosomal proteins. A band at 14k is likely to contain six essential proteins L20, L14, S12, S11, S8, and L17 with molecular weight ranging from 13.50 to 14.37 between S19 (13.13) and S9 (14.86). The 14k band density can be more exactly measured if compared with the other crowding bands in the range of 10-20k (Fig. 6), suggesting that this band's density may be proportional to the amount of S10-GFP polypeptide. Although this is a rough estimate, the observed ratios of fluorescence intensities of S10-GFP protein to the densities of 14k band at the time points from 6 h to 48 h in the same gels (Fig. 7A), were nearly constant from 6 h to 24 h. There is a little decrease after 36 h, which could be interpreted as the relative increase of the contaminating proteins in the 14k band to ribosomal proteins due to the decreased level of ribosomes in this period, as described later. Fluorophore maturation seems to be

completed in stationary phase, since otherwise the ratio would be expected to increase according to the culture time. For the four other strains used in this study, similar constant ratios were observed (Fig.7B-E) when ribosomes had not been significantly digested (Fig.8 and 9), indicating the completed maturation.

The S10-GFP or S2-GFP protein in the forms of ribosomes and aggregates

In literature, polyacrylamide or its composite gels were used to separate various forms of ribosomes (Dahlberg *et al.*, 1969). However when crude cell extracts are electrophoresed in the presence of acrylamide, non-ribosomal proteins contaminate the ribosomal bands. If the acrylamide is omitted, ribosomes move ahead of the single proteins in agarose (Gausing, 1974). In our study, it was critical to distinguish S10-GFP in the form of ribosome and the free S10-GFP protein. Therefore, we used 2% agarose gel electrophoresis to separate ribosomal particles from the free S10-GFP protein in the cytosolic fraction of the crude cell extract, while running the same extract on SDS-polyacrilamide gel to measure the total S10-GFP. 2% agarose has too low resolution to separate the forms of 70S and 100S, and they migrate to form a single major band. Under these condition, the cytoplasmic fraction of S10-GFP strain showed single bands in agarose gel (Fig. 8A left). For this strain, the fluorescence intensities of the bands in agarose and polyacrylamide gels were similar at most time points (Fig. 8B), showing that most of the S10-GFP peptide exists as a subunit of ribosome in this strain.

In contrast, there are faint but significant minor bands with smaller mobilities in agarose gel electrophoresis for all other examined strains (Fig. 8A right). The same mobility of 70S and 100S in the agarose gel electrophoresis suggests that the mobility is determined by the ratio of charge to mass rather than only by the mass. These minor bands suggest the existence of heterogeneous forms of ribosomes or aberrant ribosomes in strains with altered 100S formation, probably due to the loss of nucleic acids, and/or binding of positive polymers as well as proteins of large mass. The intensity of the major band in agarose gel was about 50-90% of that in the SDS polyacrylamide gel electrophoresis. The total intensity in agarose gel was not significantly different from that in the SDS-PAGE for any of the strains examined (Figs. 8C-F). For all examined strains, most the of GFP-fused S10 or S2 polypeptides in the cytoplasmic fraction migrate as large nucleoprotein complexes in agarose. Therefore, the absence of 100S

(S2-GFP, S10-GFPΔ*rmf*, and S10-GFPΔ*hpf)*, as well as the absence of the dissociation of 100S at the correct timing (S10-GFPΔ*yfiA),* generates the heterogeneous ribosomes. In other words, the homogeneity of ribosomes is maintained by the correct timing of 100S formation but not simply by the presence of 100S.

In all the 5 strains, the highest level of cytosolic S10-GFP in both agarose and polyacrylamide was observed at 12 h. In S10-GFP there was a plateau up to 30 h, while in all the other mutants there was no plateau and the level of S10-GFP was decreasing after 12 h.

To follow the temporal changes of S10-GFP included in the aggregate fraction, the pellets left after the extraction of the cytosolic fraction were subjected to another extraction, this time with an SDS-containing buffer. The fluorescence intensity of S10-GFP protein was stable in SDS polyacrylamide gel if the extraction was performed in the presence of 15% glycerol in a buffer conditioning 0.5% SDS at room temperature (Table III-2) or at 37°C (Table III-3), although a 6xHis-tagged GFP not fused to other proteins showed significant sensitivity to SDS under the same conditions (data not shown). Another significant factor that could influence the yield of extraction could be the absence of reducing reagent in the extraction buffer. We compared the amounts of the extracted proteins in the presence and absence of 10 mM DTT by quantitation with staining with Coomassie Brilliant Blue. Addition of DTT did not improve the extraction of proteins near 14k (Table III-4), validating the comparison between the cytoplasmic and the solubilized aggregate fractions by fluorescence.

The fluorescence intensities of the aggregate fractions solubilized in SDS-containing buffer were plotted with those of the cytoplasmic fraction against culture time (Fig. 9). The aggregate fractions for all the examined strains at the major time points were less than 20% of those of the cytosol fractions, except for S10-GFPΔ*rmf* in later hours. This indicates that intact ribosomes are not stored as aggregates during their degradation, suggesting a straightforward degradation to oligo peptides. This finding is consistent with the finding that ribosomal proteins in aggregates are mostly in aberrant forms (Maisonneuve *et al.*, 2008). For S10-GFPΔ*rmf*, the aggregate fraction is almost constant up to 48 h and its level is as high as 40% of the cytoplasmic fraction at 48 h or later. Though the data presented in Fig.9 was corrected for the extraction yield (Table V), it was still possible that the amount of S10-GFP in

the aggregate fraction was overestimated: it may contain up to 7% of the soluble S10-GFP due to only washing the pellet once (See Table V). The intensities of the aggregate fraction, corrected for the contamination with proteins from soluble fraction, are shown in Fig.10. In all strains, except for S10-GFP*Δrmf*, the intensities of the aggregated fraction seem to be decreasing gradually. In S10-GFP*Δrmf*, the level of fluorescent protein in the aggregate fraction remains constant during the whole period of 60 h examined, and at an almost twice the level observed in other strains. Therefore, the tendency is the same as can be observed in the Fig.9, but after the correction the difference between S10-GFP*Δrmf* and other strains becomes more pronounced. This suggests a contribution of RMF in preventing the accumulation of aggregates.

We also did a microscopic examination of cells of all the five studied strains at 7, 18, 30 and 60 h of culturing (Fig. 12). The 7 h time point was chosen over 6 h because S10-GFP*Δrmf* and S10-GFP*Δhpf* have a time-lag in their growth, and at 6 h the images of the cells of these two strains would correspond to approximately 3-4 h of growth of other 3 strains. By 7 h in all the 5 strains the distribution of ribosomes in the cytoplasm becomes homogeneous. The observed localization of fluorescent protein in the majority of the cells at each chosen time was consistent with the time-course of cytoplasmic and aggregate fractions in polyacrylamide gel (Fig.9). Namely, at the time points of significant decrease of the fluorescence in the cytoplasmic fraction as measured by SDS-PAGE (Fig. 9), the relative decrease of the cytoplasmic fluorescence comparing to the poles was observed during the microscopic examination. Notably, for all 5 strains even at 60 h there was a small population of cells remaining with no foci and homogeneous fluorescence spread all over the cell, suggesting that divergence of the cell fate occurs in the period when no foci can be observed, and in a small group of cells aggregate formation and degradation of ribosomes do not occur at the same rate as they do in the majority of the cells.

Time course changes of CFU

The amount of viable cells in a bacterial culture is commonly estimated as a number of colony forming units (CFU) per volume of liquid culture. To clarify the relationship between protein turnover and viability, we measured the CFU count more accurately

than that by the conventional spreading method. We noticed that spreading *E. coli* cells on an agar plate only partially dissociates the cell clusters that are formed in stationary phase. Due to this defect, the CFU count is significantly underestimated and becomes less reproducible. Therefore, we modified the classic dilution-mixing method to measure CFU (see Experimental Procedures). By this method, vortexing dissociates the cell clusters reproducibly and errors can be minimized almost to the level of pipetting error.

The S10-GFP strain behaved similarly to the wild-type W3110 (Fig. 12A), and thus it was additionally confirmed that the fusion of S10 with GFP did not affect the viability. The other mutant strains began to decay earlier than those of S10-GFP irrespective of whether the mutation blocked the formation (Figs. 12C-E) or the dissociation of 100S (Fig. 12F). Except for S10-GFP, there were no plateaus after 12 h, meaning the absence of stationary phase after 12 h. The most rapid decay was observed for S2-GFP.

Interestingly, S10-GFPΔ*yfiA* strain, which has the highest and persistent level of 100S accumulation among the examined strains (Fig. 4 E,G), showed the second most rapid decay, while the other two disruptants showed slower decays. In other words, the phenotypes cannot be straightforwardly explained by a single presumable function of 100S such as conferring resistance against degradation or providing a better substrate for producing amino acids.

Notably, the CFU count is proportional to S10- or S2-GFP band intensities, as determined by SDS-PAGE, suggesting a constant level of ribosomes in a viable cell in decay period. Exceptionally, the CFU value of S10-GFPΔ*rmf* (Fig. 12D) is somewhat smaller than could be expected from the S10-GFP intensity in SDS polyacrylamide, comparing to other strains.

Effect of addition of amino acids on CFU

In decay period, it is possible that cell death is dependent on the available amounts of amino acids, i.e. its rate increases when amino acids become deficient. To examine this possibility, we added 20 amino acids to a culture at various time points and further cultured for 12 h. The control culture was similarly cultured with no addition of amino

acids, and the ratio of CFU with the addition to CFU with no addition was calculated. If the deficiency of amino acids causes cell death at a particular time, the ratio at that time point will be larger than 1.

The obtained ratios were dependent on the strains and the time points (Fig. 13). For S10-GFP, the addition of amino acids had no effect in stationary phase, 12 h and 24 h, but increased the CFU values 1.5-fold at 36 h when rapid decay was observed (Fig. 12B). Furthermore, S2-GFP and S10-GFPΔ*yfiA* strains, which showed rapid decay from 12 h and 24 h (Figs. 12C and 12F), showed significantly reduced cell death following addition of amino acids from 12 h and 24 h, respectively. These results demonstrate that the deficiency of amino acids is one of the major causes of cell death during the rapid decays in decay period. In contrast, the other two strains, showing relatively slow decays (Figs. 12D and 12E), demonstrated no effects at 12 h and 24 h but modest ones at 36 h, suggesting a difference in the protein turnover among the three strains lacking 100S (S2-GFP vs S10-GFP *Δrmf* and S10-GFP *Δhpf*).

Discussion

The role of 100S in protein turnover

The role of *E. coli* 100S ribosomes was proposed to be a hibernation form of ribosomes as a storage of intact ribosomes (Yoshida *et al.*, 2002). This proposal is based on the quick dissociation of 100S into translationally active 70S upon addition of fresh rich medium to a stationary culture (Wada *et al.*, 1990). Under these conditions, *rmf* mRNA is significantly degraded within 1 min, and 100S disappears, as determined by the density gradient analysis of crude extract of cells harvested at 1 min (Aiso *et al.*, 2005). Therefore, 100S surely works as a storage of hibernating ribosomes.

However, these results do not exclude other potential roles for 100S ribosomes. In LB medium, 100S is significantly expressed for only a short period in stationary phase (Fig. 4A), and thus cannot work as a storage after 18 h. However, only S10-GFP, which is the closest to wild type, displays stationary phase up to 30 h, and other strains have shorter stationary phases irrespective of inhibited or enhanced formation of 100S. Therefore, the results indicate that the timing of 100S formation and breakdown is more critical for the longer stationary phase than the existence of 100S itself. This suggests that 100S is a repository of ribosomes that tentatively protects ribosomes from degradation and is later degraded to produce amino acids.

Strictly speaking, cell death and the formation of 100S may be two independent and unrelated phenomena sharing a common cause. However, there is a circumstantial evidence for the repository model of 100S. Firstly, time course changes of the CFU count and the residual level of ribosomes are similar (Fig.12), suggesting a close relationship between ribosome degradation and cell death. Secondarily, the results of the experiment shown in Fig.13 claim that cell death, at least the rapid one, is controlled by the available amounts of amino acids in decay period, suggesting the importance of protein turnover. Thirdly, ribosome degradation is the largest source of amino acids.

Whether or not the formation of 100S protects ribosomes from degradation is the key hypothesis to interpret the results obtained in this study. Since the formation prevents ribosomes from dissociating into 50S and 30S, which are good substrates for degradation (Zundel *et al.*, 2009), the formation must increase the resistance to degradation as a whole, unless 100S ribosomes themselves are very susceptible to

degradation. According to the protection hypothesis, ribosomes of S2-GFP, S10-GFPΔ*rmf*, and S10-GFPΔ*hpf,* which are all unable to form 100S, should be degraded more than those of S10-GFP, while in S10-GFPΔ*yfiA*, which shows a more persistent 100S formation, ribosomes should be degraded less than in S10-GFP. However, the observed results are different from this prediction, suggesting the presence of more factors to be considered.

One of such factors is the protein turnover. In the presence of amino acids, ribosomes would be regenerated through translation as observed for the quality control of rRNA (Basturea et al., 2011). If the amino acids are deficient, free 30S and 50S particles are likely to be degraded. In the absence of amino acids, the degradation would be thus compensated by the regeneration, and their balance controlled by 100S and the proper time of its dissociation can explain the plateau of the ribosome level up to 30 h for S10-GFP (Fig 8B). This is further supported by the fact that S10-GFP is not starved for amino acids at 12 h and 24 h (Fig. 13). When no 100S is formed, concentrations of amino acids in late stationary phase would be simply decreasing in time according to the consumption of proteins, and thus decreasing the regeneration, resulting in a peak of ribosome level with no plateau as observed for S2-GFP, S10-GFPΔ*rmf*, and S10-GFPΔ*hpf* (Fig. 8).

These considerations can be applicable also to the behavior of S10-GFPΔ*yfiA*. If 100S is neither degraded nor regenerated at nearly 12 h, the level of ribosomes should show a peak and a decrease, according to the decrease of the regeneration due to the consumption of proteins and ribosomes other than 100S. Since there is no difference from S10-GFP before the accumulation of YfiA in S10-GFP, it should behave the same as S10-GFP up to the peak, while the level of ribosomes should decrease due to the absence of regeneration. All these features were actually observed. Furthermore, the hypothesized absence of degradation of 100S was evidenced by the deficiency of amino acids at 24 h (Fig. 13). In contrast, in S10-GFP where YfiA dissociates 100S, 100S is no longer protected from degradation and regeneration of ribosomes is maintained by the protein turnover, maintaining stationary phase much longer than in S10-GFPΔ*yfiA*. Consistently, there was no deficiency of amino acids at 24 h for S10-GFP (Fig. 13).

This is the speculated answer for why the observed time courses of the level of ribosomes are almost similar or homothetic among the four strains but different from

that of S10-GFP showing a plateau.

Therefore, we propose a model, where 100S ribosome in *E.coli* plays at least two different roles in the early and later stationary phase, namely, it protects ribosomes from degradation at the earlier stage and provides the cell with amino acids in the later stage (Fig. 14, Model A). These two functions of 100S may have evolved from the bifunctional property of ribosome as a protein-synthesizing machine and the largest source of amino acids.

While Model A (Fig. 14, Model A) is based on a hypothesis that 100S is more resistant to degradation than the rest of the ribosomal particles, there is not enough evidence to dismiss a possibility that 100S could be especially susceptible to degradation. It may seem counterintuitive, but in fact, in the studies of cold shock, YfiA-bound 70S ribosomes are known to be translationally inactive (Thieringer et al., 1998). And, as YfiA binds to ribosomes more tightly than either RMF or HPF, it is not unreasonable to suppose that 100S could be easier dissociated than YfiA-bound 70S. If we suppose that 100S is less resistant to degradation than 70S ribosomes (YfiA-bound or not, here we don't have data to distinguish between these types), it is also possible to explain the results obtained in this study. We propose this as Model B (Fig. 14, Model B).

According to Model B, in S10-GFP, at first 100S will be preferentially degraded, increasing the pool of amino acids, and therefore the degradation will be compensated by regeneration. When all 100S is degraded, the rate of both degradation and regeneration will decrease, but the remaining size of the amino acid pool will still allow the cell to balance degradation with regeneration. When the amino acids supplied by protein turnover become deficient, the rapid decay occurs at 36 h. In contrast, in S10-GFP*ΔyfiA,* extensive formation of 100S will lead to excessive degradation, and the amino acid pool will be used by 24 h, where the rapid decay occurs. In S10-GFP*Δrmf* and S10-GFP*Δhpf,* where no 100S is formed, the amino acid level is simply decreasing after 12 h, therefore the regeneration is also slowly decreasing according with the consumption of proteins, resulting in a slower decay.

Contradictions with previous studies regarding the viability of *Δrmf*

There is an often cited report regarding 100S and its relation to viability, showing W3110*Δrmf* mutant to die earlier than the wild type strain (Yamagishi et al., 1993), and another study, discussing the viability of W3110*Δhpf*, W3110*ΔYfiA*, and W3110*ΔhpfΔYfiA* (Ueta et al., 2005), where no significant effect of *hpf* and *yfiA* disruption was found, though it was suggested that *ΔyfiA* might be living a little longer. While in our study, S10-GFP*Δrmf* mutant showed a shorter stationary phase, but also a slow decay, and S10-GFP*ΔYfiA* showed a fast decay with shorter stationary phase, comparing to the background S10-GFP strain.

It is, unfortunately, very difficult to compare those studies with our results due to the following considerations. Firstly, the previously used CFU counting technique is less inaccurate than the modification used in this study. Secondly, in the second study viability was presented as relative viability (CFU/OD values). As OD in stationary phase and decay period is not proportional to the number of cells it is difficult to compare the CFU/OD values with CFU values. Thirdly, in the above-mentioned studies a different medium was used, and the dynamics of 100S formation and the dynamics of cell death could be different in different media. Lastly, though GFP fusion doesn't significantly affect the growth rate (Fig. 3), it could potentially affect the susceptibility of ribosomes to degradation. Our study showed that ribosomal level and CFU decrease in parallel, therefore, if the ribosomes of a W3110*Δrmf* mutant from the study above were degraded at a faster rate, it could also result in a faster loss of viability.

Unanswered questions

There are many features revealed by the results of our study that haven't been explained. For example, why are the decays of CFU and the ribosome level so rapid for S2-GFP if compared to S10-GFPΔ*rmf* and S10-GFPΔ*hpf* in spite of their common absence of 100S? Why does only S10-GFPΔ*rmf* show the similarity of CFU time course to the amount of S10-GFP polypeptide in the major band in agarose but not to its total amount, with which the CFUs of other four strains are more correlated? These questions could potentially be addressed by introducing a different susceptibility against degradation of the YfiA-bound 70S, or by introducing additional functions of RMF, HPF and YfiA in relation to aggregate formation, or ribosomal maturation. Moreover, the susceptibility to

degradation of S2-GFP and S10-GFP-containing ribosomes may be different. Further studies are required to resolve the molecular mechanisms that modulate 100S formation and to determine its role in the stationary phase.

Experimental procedures

Strains and culture

All strains constructed were derived from W3110 and are listed in Table III. The DNA fragments harboring *rpsJ* (S10)-*gfp* and *rpsB* (S2)-*gfp* were prepared with fusion PCR (Nakayama and Shimamoto, 2014) with GGN degenerating linker (Bakshi *et al.*, 2012). The fragments replaced unfused genes with Red recombination method (Datsenko and Wanner, 2000), and the resultant genes were transferred to W3110 with P1 transduction. The deletions were obtained from Keio Clones (Baba *et al.*, 2006), and similarly transferred to the S10-GFP strain, HN3611. The antibiotic marker cassettes were removed with pCP20 (Cherepanov, Wackernagel, 1995) expressing FLP recombinase, because the antibiotic marker affects the growth rates.

B-maggio (PCT/JP2014/081308) is used for GFP. The kanamycin marker gene introduced as the marker of the deletions has been removed because it sometimes causes slow growth and low saturation level. Fluorescence of a solution was measured with a fluorescent spectrophotometer (FluoroMax-4, Horiba, Kyoto), and no optical properties of B-maggio were altered by the protein fusions.

The sequences of the selected linker connecting S10 and S2 with GFP are
S10-ATCAGCCTGGGT (C-terminus)-CAGGAAAGGCGACAGGAG-(N-terminus of B-maggio)CGTAAAGGAGAAGAA
and
S2-GTAGAAGCTGAG (C-terminus)-CAGGAAAGGCGACAGGAG-(N-terminus of B-maggio)CGTAAAGGAGAAGAA.

For identifying 30S, 50S, 70S, 90S, and 100S bands in the sucrose-gradient ultracentrifugation, we constructed a doubly labeled strain in which L27 and S10 are labeled with mCherry and B-maggio, respectively.

A strain from a single colony was grown at 37°C by inoculation into 2ml of LB Lenox and then pre-synchronized. Pre-synchronization essential for reproducibility in this study is the inoculation of 20 µl of 12 h culture into 2 ml of fresh medium, and it was repeated twice or more to establish the pre-synchronized culture.

Preparation of *E. coli* extracts and gel electrophoresis

Typically, 0.25 ml of a culture was collected in a 1.5 ml sample tube and centrifuged for

5 min at 5,000 rpm. The supernatant was discarded and the cell pellets were stored at -80□ until the samples of all time points were ready for their examination. The cell pellets were suspended in 10 µl of 10 mM Tris-HCl (pH 7.6) containing 15% glycerol, 100 mM ammonium acetate and 15 mM magnesium acetate, Buffer A, as well as ca. 30 mg of zirconium beads with 0.5 mm diameter (Atto, Tokyo). The tubes were vibrated with a mixer (Delta Mixer Se-08, TAITEC, Tokyo) at 3000 rpm for 5 min, and then centrifuged at 15,000 rpm at 4°C for 5 min. The supernatant was collected and the pellet was re-extracted with 10 µl of Buffer A followed by a vibration for 5 min and a centrifugation. The two supernatants were combined and mixed with 2 µl of 70% glycerol containing Bromophenol blue (the cytoplasmic fraction). The first two extracts contained 93% of the protein that could be extracted in 4 sequential extractions (Table V).

The residual pellet was further extracted with 10 µl of 40 mM Tris-acetate (pH 7.6) containing 1 mM EDTA, 15% glycerol and 0.5% SDS (Buffer B) at 37°C with vibration, and centrifuged at room temperature, otherwise in the same conditions. Two more extractions with 10 µl of Buffer B were repeated, and all three supernatants were combined and mixed with 2 µl of 70% glycerol containing Bromophenol blue (the solubilized aggregate fraction). The first three extracts contained 84% of the protein that could be extracted in 7 sequential extractions (Table V).

For the cytoplasmic fraction, 7 µl was analyzed with 2% agarose gel electrophoresis in Buffer A. The gel has a size of 100 mm (w)x60 mm (l)x3mm (t), and the whole horizontal electrophoresis apparatus was ice-cooled with the buffer circulated during the electrophoresis at 50 V for 1 h. Another 2 to 7 µl of the cytoplasmic fraction and the entire solubilized aggregate fraction were analyzed with Laemmli SDS gel electrophoresis with a modification that the separation gel buffer in 12% polyacrylamide were replaced by Wide-Range-Gel (Nacalai Tesque, Kyoto).

Quantitation of S10-GFP protein in electrophoretic gels by fluorescence

The agarose or polyacrylamide gels were laid on a black background surface and irradiated with a 15W blue LED lamp (MR-15LED-E, LLC GBAM, Tokyo) set approximately 130 cm away from the gel at an angle of about 45° in a dark room. Images were obtained with a camera through two long-pass filters of 530 nm (Toshiba,

Tokyo) and 540 nm (Atto, Tokyo). An integrated fluorescence intensity was quantified with ImageJ (NIH, Bethesda).

The intensity of the LED lamp decreases with time (Fig.15), therefore each photo was taken immediately after turning the LED lamp on, and the exposure time was set to no more than 10s. The optimal distance from the lamp to the gel was experimentally chosen because of the following considerations: if it was set too far, longer exposure time was needed to take a photograph, but if it was set too close, the distribution of the excitation light over the surface of the irradiated gel was becoming too inhomogeneous. Table 6 shows the inhomogeneity of the light over the surface measured with the LED lamp set at 130 cm away from the surface. It was no more than 16%. When the same sample was loaded in 8 wells on the same gel and the band intensities were measured, the error was calculated to be 5.4% before correction for inhomogeneity of the light (Table 1-2) and 6.1% after the correction (Table 1-3), therefore the error introduced by the inhomogeneity of the light was considered to be negligible, and in the routine analysis of the photos the correction for the inhomogeneity of the light was not conducted. Table 1-1 also shows that 5 minutes of continuous irradiation of the gel in the described conditions did not decrease the measured intensity of B-Maggio fluorescence.

Quantitation of protein in Coomassie Brilliant Blue stained electrophoretic gels

When the fluorescent images had been obtained, the gels were then stained with Coomassie Brilliant Blue (Pink *et al.*, 2010) after their fluorescent images were photographed. A stained gel was scanned with a transmittance scanner (GTX-800, Epson, Tokyo). The resulting image was coded in a log color space, therefore it had to be converted to linear color space to ensure that the optical density of the image was proportional to the amount of quantitated protein. The conversion was done in the 32-bit format with ImageJ software (NIH, Bethesda) according the following formula:

$$OD = -1 * 1.8 * \ln(value/65536) / \ln 10,$$

Where 1.8 is a default gamma of the EPSON scanner. The converted image was analyzed with ImageJ (NIH, Bethesda). The amount of proteins was obtained by using a calibration curve obtained from the standard band densities of various volumes of 1 mg/ml BSA (Thermo Scientific, Illinois).

Ultracentrifugation

The cell extracts were prepared from the wet cells similarly as written above. The amounts of cultures, beads, and the volume of Buffer A were increased by eight folds. Since cell extracts were exposed to longer periods at room temperature, Buffer A contained protease inhibitors of 0.2 mM of phenylmethanesulfonyl fluoride and EDTA-free cOmplete (Rosh, Mannheim). The cells were lysed by vibration at 3,000 rpm with a bead crusher μT-12 (TAITEC, Tokyo) for 5 min. The lysed cells were centrifuged at 15,000 rpm for 5 min at 4°C. The supernatant was transferred into a new sample tube and further centrifuged under the same condition to remove any residual beads. The supernatant was layered on a 5–20% sucrose density gradient in Buffer A, and centrifuged in a SW40 rotor (Beckman, Fullerton) at 25,000 xg for 1.5 h at 4° C. The sucrose density gradients had been made with a gradient maker (GRADIENT MATE 6T, Biocomp Instruments, Fredericton), and the program is shown in Table VII. After the centrifugation, photos were taken by irradiating with blue LED lamp array SPV-220 (Oriental Instruments, Sagamihara) through the long-pass filters.

CFU measurements

At each time point, a culture was vigorously vortexed, and 1~100 μl containing less than 2000 viable cells was added to a 0.5 ml of LB which had been prespotted at a semicircle of a polystyrene petri dish with a diameter of 90 mm. Autoclaved water was sprayed on the plate, and then 2.5 mL of 0.5% agar (Spoon Agar, Mitsui Sugar, Tokyo) which had been kept at 50°C was placed at the opposite semicircle so that the cells were not directly heated. After waiting for 3-7 s until partial gelation started, the solutions were mixed with a gentle horizontal shaking of the plate. The presence of gel fragments during the mixing was allowed as a guarantee of a low enough temperature. The spraying water facilitated spreading of the mixture to cover the whole dish bottom. This plating requires a certain quality of agar which gelates slowly at around 37°C but forms a homogeneous solution at 50°C.

The plates were incubated at the shortest for 24 h at 37°C, because the cells which have sunk to the bottom of the plate take a longer time to form distinguishable colonies than those at the surface. Another 24 h incubation did not significantly increase

the measured values of CFU. They were photographed with a camera positioned at 50 cm above the plate which was homogeneously illuminated from the position 25 cm below to contrast the tiny colonies. The photo pixel corresponded to 30 μm x 30 μm on the plate surface, and an area bigger than 20 pixels was recognized as a colony in a homemade ImageJ macro application. Since most petri dishes have marks, which could be incorrectly counted as colonies, an empty agar plate was photographed and the background number, usually 15-30, was subtracted. This procedure can count colonies up to 2500 per plate without any saturation (Fig.16).

Acknowledgements

First of all, I am grateful to my supervisor, Prof. Nobuo Shimamoto, for help, patience, advice, critique, and providing the insightful information on the importance of taking into account what the reader/listener is thinking, and overall about the Japanese mentality. I also greatly thank Dr. Hideki Nakayama for help, discussions and valuable advice regarding experimental work and food. I also thank all the members of the Journal Club at Osaka Medical University, and I especially appreciate all the insightful information I learnt from Dr. Yoshida Hideji, Dr. Akira Wada, Dr. Chieko Wada, and Dr. Masami Ueta.

References

Adam, V., Carpentier, P., Violot, S., Lelimousin, M.I., Darnault, C., Nienhaus, G.U., and Bourgeois , D. (2009). Structural Basis of X-ray-Induced Transient Photobleaching in a Photoactivatable Green Fluorescent Protein. J.Am.Chem.Soc. 131, 18063-18065

Aiso, T., Yoshida, H., Wada, A., and Ohki, R. (2005). Modulation of mRNA stability participates in stationary-phase-specific expression of ribosome modulation factor. J. Bacteriol. 187, 1951–1958.

Auerbach, D., Klein, M., Franz, S., Carius, Y., Lancaster, C.R.D., and Jung, G. (2014). Replacement of highly conserved E222 by the photostable non-photoconvertible histidine in GFP. Chembiochem 15, 1404–1408.

Baba, T., Ara, T., Hasegawa, M., Takai, Y., Okumura, Y., Baba, M., Datsenko, K.A., Tomita, M., Wanner, B.L., and Mori, H. (2006). Construction of Escherichia coli K-12 in-frame, single-gene knockout mutants: the Keio collection. Mol. Syst. Biol. 2, 2006.0008.

Bakshi, S., Siryaporn, A., Goulian, M., and Weisshaar, J.C. (2012). Superresolution imaging of ribosomes and RNA polymerase in live Escherichia coli cells. Mol. Microbiol. 85, 21–38.

Basturea, G.N., Zundel, M.A., and Deutscher, M.P. (2011). Degradation of ribosomal RNA during starvation: Comparison to quality control during steady-state growth and a role for RNase PH. RNA 17, 338–345.

Ben-Hamida, F., and Schlessinger, D. (1966). Synthesis and breakdown of ribonucleic acid in Escherichia coli starving for nitrogen. Biochimica Et Biophysica Acta (BBA) - Nucleic Acids and Protein Synthesis 119, 183–191.

Bremer, H., and Dennis, P.P. (1996). Modulation of chemical composition and other parameters of the cell by growth rate. Escherichia coli and Salmonella: Cellular and Molecular Biology 2, 1553–1569.

Cherepanov, P.P., and Wackernagel, W. (1995). Gene disruption in Escherichia coli: TcR and KmR cassettes with the option of Flp-catalyzed excision of the antibiotic-resistance determinant. Gene 158, 9–14.

Dahlberg, A.E., Dingman, C.W., and Peacock, A.C. (1969). Electrophoretic characterization of bacterial polyribosomes in agarose-acrylamide composite gels. J. Mol. Biol. 41, 139–147.

Datsenko, K.A., and Wanner, B.L. (2000). One-step inactivation of chromosomal genes in Escherichia coli K-12 using PCR products. Proc. Natl. Acad. Sci. U.S.A. 97, 6640–6645.

Davis, B.D., Luger, S.M., and Tai, P.C. (1986). Role of ribosome degradation in the death of starved Escherichia coli cells. J. Bacteriol. 166, 439–445.

Finkel, S.E. (2006) Long-term survival during stationary phase: evolution and the GASP phenotype. Nature Reviews 4, 113-119

García-Fruitós, E., González-Montalbán, N., Morell, M., Vera, A., Ferraz, R.M., Arís, A., Ventura, S., and Villaverde, A. (2005) Aggregation as bacterial inclusion bodies does not imply inactivation of enzymes and fluorescent proteins. Microbial Cell Factories 4:27.

Gausing, K. (1974) Ribosomal Protein in *E.coli:* Rate of Synthesis and Pool Size at Different Growth Rates. Molec. gen. Genet. 129, 61-75.

Habuchi, S., Cotlet, M., Gensch, T., Bednarz, T., Haber-Pohlmeier, S., Rozenski, J., Dirix, G., Michiels, J., Vanderleyden, J., Heberle, J., De Schryver, F.C., and Hofkens, J. (2004) Evidence for the Isomerization and Decarboxylation in the Photoconversion of the Red Fluorescent Protein DsRed. J.Am.Chem.Soc. 127, 8977-8984.

Ito, Y.Y., Suzuki, M.M., and Husimi, Y.Y. (1999). A novel mutant of green fluorescent protein with enhanced sensitivity for microanalysis at 488 nm excitation. Biochem. Biophys. Res. Commun. 264, 5–5.

Kane, J.F., and Hartley, D.L. (1988). Formation of recombinant protein inclusion bodies in Escherichia coli. Trends in Biotech. 6, 95–101.

Kato, T., Yoshida, H., Miyata, T., Maki, Y., Wada, A., and Namba, K. (2010). structure of the 100S ribosome in the hibernation stage revealed by electron cryomicroscopy. Structure 18, 719–724.

Keener, J., and Nomura, M. (1996) Regulation of ribosome synthesis. *Escherichia coli* and *Salmonella*: cellular and molecular biology, 2nd ed. ASM Press, Washington, DC, 1417-1431.

Koch, A.L., and Levy, H.R. (1955). Protein turnover in growing cultures of Escherichia coli. J. Biol. Chem. 217, 947–957.

Kopito, R.R. (2000). Aggresomes, inclusion bodies and protein aggregation. Trends Cell Biol. 10, 524–530.

Maisonneuve, E., Fraysse, L., Moinier, D., and Dukan, S. (2008). Existence of abnormal protein aggregates in healthy Escherichia coli cells. J. Bacteriol. 190, 887–893.

Maki, Y., Yoshida, H., and Wada, A. (2000). Two proteins, YfiA and YhbH, associated with resting ribosomes in stationary phase Escherichia coli. Genes Cells 5, 965–974.

McCarthy, B.J. (1962). The effects of magnesium starvation on the ribosome content of Escherichia coli. Biochimica Et Biophysica Acta (BBA) - Specialized Section on Nucleic Acids and Related Subjects 55, 880–889.

Nagai, T., Ibata, K., Park, E.S., Kubota, M., Mikoshiba, K., and Miyawaki, A. (2002). A variant of yellow fluorescent protein with fast and efficient maturation for cell-biological applications. Nat. Biotechnol. 20, 87–90.

Nakayama, H., and Shimamoto, N. (2014). Modern and simple construction of plasmid: Saving time and cost. J. Microbiol. 52, 891–897.

Needham, M., and Mastaglia, F.L. (2007). Inclusion body myositis: current pathogenetic concepts and diagnostic and therapeutic approaches. The Lancet Neurology 6, 620–631.

Piir, K., Paier, A., Liiv, A., Tenson, T., and Maiväli, Ü. (2011). Ribosome degradation in growing bacteria. EMBO Rep. 12, 458–462.

Pink, M., Verma, N., Rettenmeier, A.W., and Schmitz-Spanke, S. (2010). CBB staining protocol with higher sensitivity and mass spectrometric compatibility. Electrophoresis 31, 593–598.

Rajan, R.S., Illing, M.E., Bence, N.F., and Kopito, R.R. (2001). Specificity in intracellular protein aggregation and inclusion body formation. Proc. Natl. Acad. Sci. U.S.A. 98, 13060–13065.

Shaner, N.C., Campbell, R.E., Steinbach, P.A., Giepmans, B.N.G., Palmer, A.E., and Tsien, R.Y. (2004). Improved monomeric red, orange and yellow fluorescent proteins derived from Discosoma sp. red fluorescent protein. Nat. Biotechnol. 22, 1567–1572.

Shaner, N.C., Lin, M.Z., McKeown, M.R., Steinbach, P.A., Hazelwood, K.L., Davidson, M.W., and Tsien, R.Y. (2008). Improving the photostability of bright monomeric orange and red fluorescent proteins. Nat. Methods 5, 545–551.

Shimomura, O. (1979). Structure of the chromophore of Aequorea green fluorescent protein. FEBS Lett. 104, 220–222.

Stepanenko, O.V., Stepanenko, O.V., Shcherbakova, D.M., Kuznetsova, I.M., Turoverov, K.K., and Verkhusha, V.V. (2011). Modern fluorescent proteins: from chromophore formation to novel intracellular applications. BioTechniques 51, 313–327.

Stewart, E.J., Madden, R., Paul, G., and Taddei, F. (2005) Aging and Death in an Organism That Reproduces by Morphologically Symmetric Division. PLOS Biology 3, 0295-0300

Thieringer, H. A., Jones, P. G., and Inouye, M. (1998). Cold shock and adaptation. Bioessays, 20(1), 49-57.

Ueta, M., Yoshida, H., Wada, C., Baba, T., Mori, H., and Wada, A. (2005). Ribosome binding proteins YhbH and YfiA have opposite functions during 100S formation in the stationary phase of Escherichia coli. Genes Cells 10, 1103–1112.

Ueta, M., Ohniwa, R.L., Yoshida, H., Maki, Y., Wada, C., and Wada, A. (2008) Role of HPF (Hibernation Promoting Factor) in Translational Activity in *Escherichia coli*. J. Bichem. 143, 425—433

Ueta, M., Wada, C., Daifuku, T., Sako, Y., Bassho, Y., Kitamura, A., Ohniwa, R., Morikawa, K., Yoshida, H., Kato, T., Miyata, T., Namba, K., and Wada, A. (2013) Conservation of two distinct types of 100S ribosome in bacteria. Genes to Cells 18, 554—574.

Wada, A., Yamazaki, Y., Fujita, N., and Ishihama, A. (1990). Structure and probable genetic location of a "ribosome modulation factor" associated with 100S ribosomes in stationary-phase Escherichia coli cells. Proc. Natl. Acad. Sci. U.S.A. 87, 2657–2661.

Yamagishi, M., Matsushima, H., Wada, A., Sakagami, M., Fujita, N., and Ishihama, A. (1993). Regulation of the Escherichia coli rmf gene encoding the ribosome modulation factor: growth phase- and growth rate-dependent control. Embo J. 12, 625–630.

Yoshida, H., Maki, Y., Kato, H., Fujisawa, H., Izutsu, K., Wada, C., and Wada, A. (2002). The ribosome modulation factor (RMF) binding site on the 100S ribosome of Escherichia coli. J. Biochem. 132, 983–989.

Yoshida, H., and Wada, A. (2014) The 100S ribosome: ribosomal hibernation induced by stress. WIREs RNA 5, 723–732.

Zambrano, M.M., and Kolter, R. (1993) Escherichia coli mutants lacking NADH dehydrogenase I have a competitive disadvantage in stationary phase. Journal of bacteriology 175, 5642-5647.

Zundel, M.A., Basturea, G.N., and Deutscher, M.P. (2009). Initiation of ribosome degradation during starvation in *Escherichia coli*. RNA 15, 977–983.

Illustrations

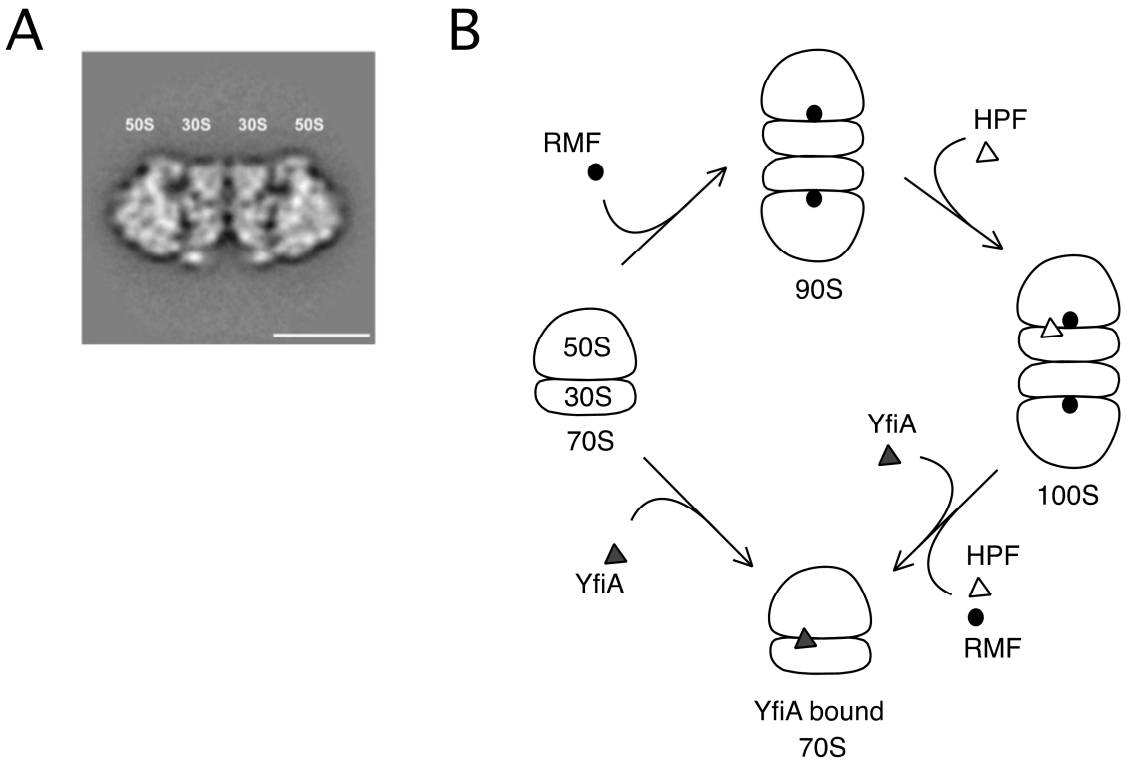

Figure 1. 100S and related factors RMF, HPF and YfiA in stationary phase.

A. Electron Cryomicrograph of a 100S ribosome (taken from Kato et al., 2010). Scale bar represents 20nm. B. Model of 100S formation in stationary phase by interacting with RMF, HPF and YfiA. RMF dimerizes 70S into 90S. HPF promotes formation of 100S. YfiA promotes dissociation (or inhibits association) of 100S. YfiA is mainly found in 70S particles. HPF is found in 100S particles exclusively.

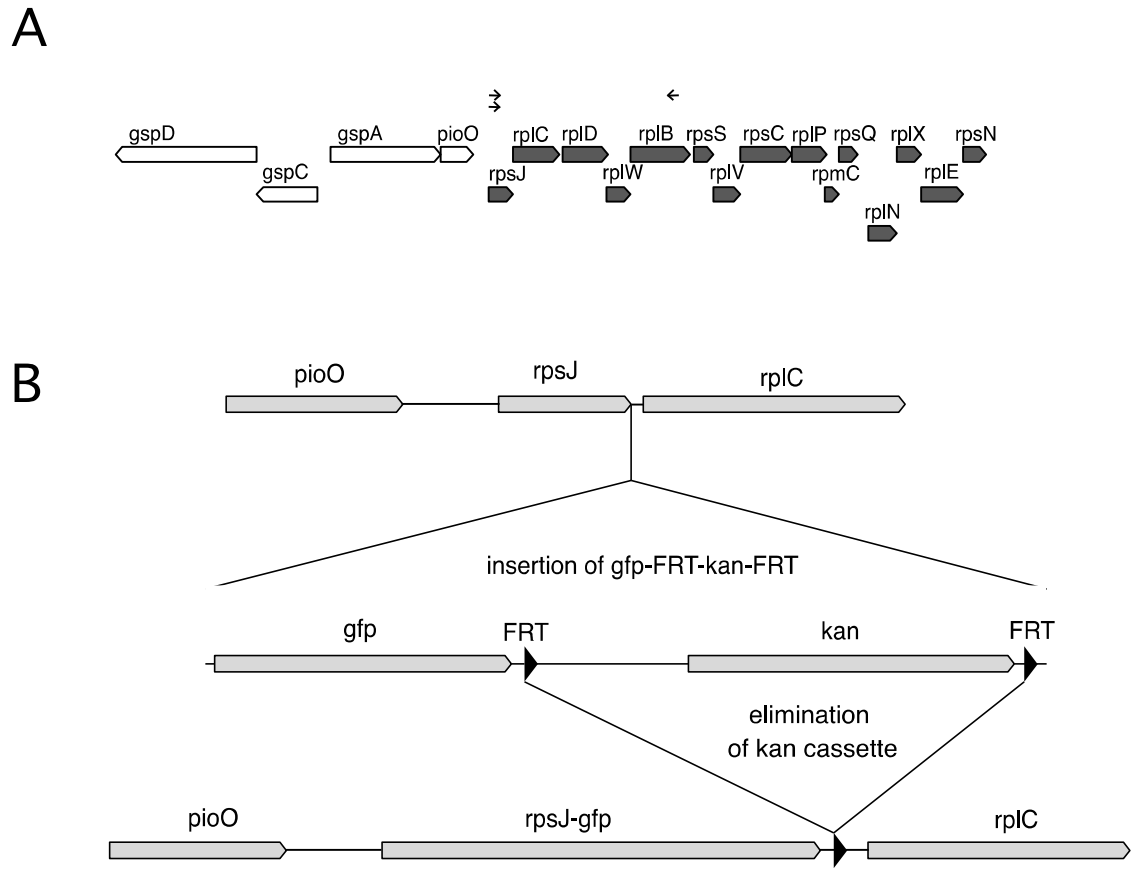

Fig. 2. Construction of S10-GFP fusion.

A. Gene map of the chromosomal region in the vicinity of *rpsJ* (adapted from SHIGEN database). Essential genes are shown in dark color, non-essential are shown in white; arrowheads indicate promoters. B. Close-up of the *rpsJ* region. *Gfp-FRT-kan-FRT* cassette was inserted directly downstream of *rpsJ*. The kanamycin resistance cassette was then removed with pCP20 plasmid. FRT regions are the recombination sites.

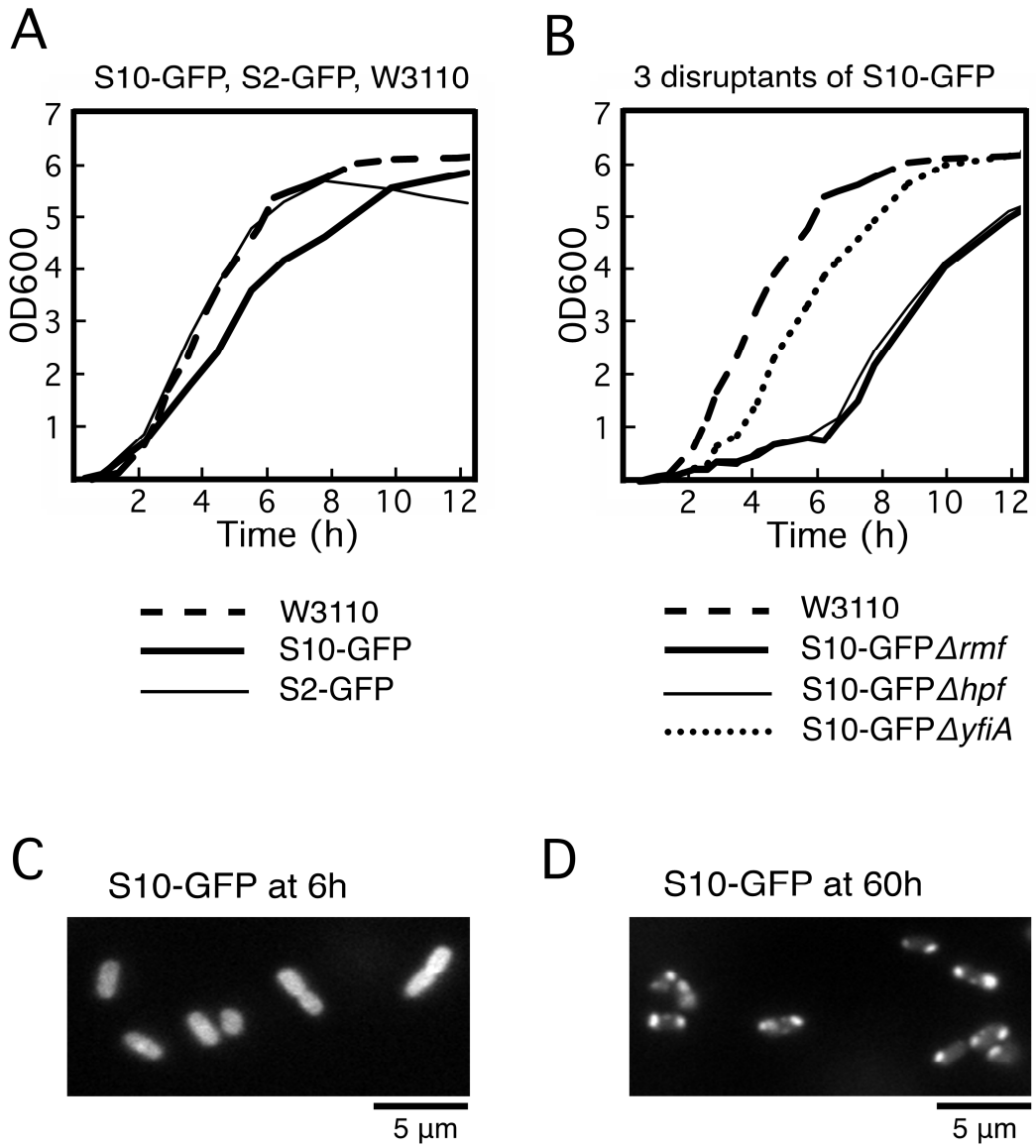

Figure 3. Growth curves and the microscopic images.

A and B. Time course of OD_{600} for W3110, S10-GFP, S2-GFP, S10-GFPΔ*rmf*, S10-GFPΔ*hpf*, S10-GFPΔ*yfiA*. The styles of lines assigned to each strain are shown below each panel. Note that the plots are linear but not semi-log. C and D. Fluorescent images of S10-GFP at 6 h (C) and 60 h (D).

Table I. Error introduced by measurements of GFP fluorescence with a LED lamp as a source of excitation light.

	Details of measurements	Fluorescence intensity			Error (%)
1	Measured for 10 s before 5 m irradiation	12.4	±	0.8	6.8%
2	Measured for 10 s after 5 m irradiation	12.1	±	0.7	5.4%
3	Measurements in (2) were corrected for the inhomogeneity of the excitation light	12.3	±	0.8	6.1%

The same sample of S10-GFP 12 h crude extract (cytoplasmic fraction) was loaded into 8 wells. In (1) gel was photographed for 10 s immediately after turning on the excitation light. In (2) the excitation light was left on for 5 m, then it was switched off, turned on again and another photograph was taken. Fluorescence intensity was measured with ImageJ (NIH, Bethesda), and its value is displayed in au. In (3) values, obtained in (2) were corrected for the inhomogeneity of the excitation light, measured from an image of a white sheet of paper, taken with the same setting of the LED lamp. Error is the SD displayed as percentage of the average.

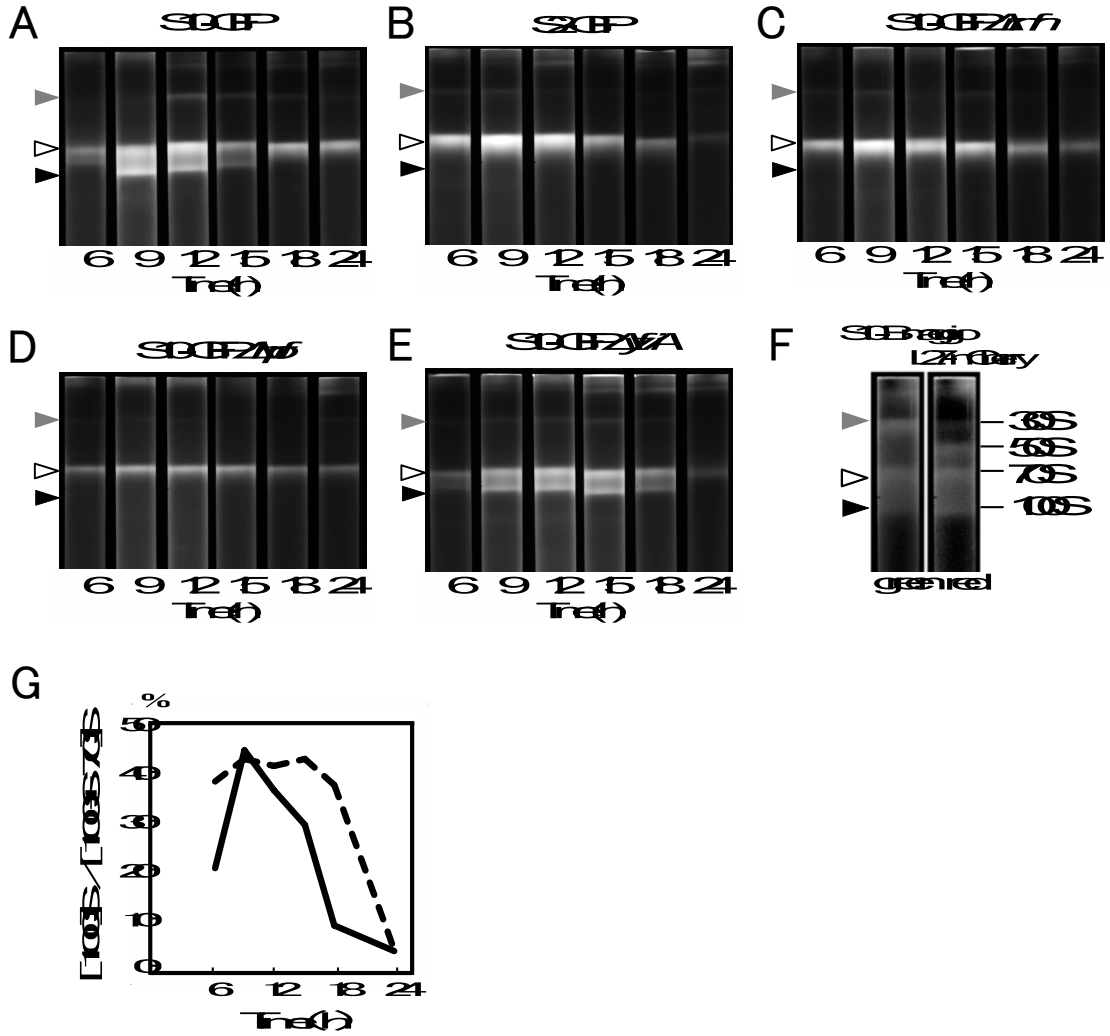

Figure 4. 100S formation.

A-E. The ribosome profiles of S10-GFP (A), S2-GFP (B), S10-GFPΔ*rmf* (C), S10-GFPΔ*hpf* (D), S10-GFPΔ*yfiA* (E). F. The ribosome profile of the marker ribosome, in which S10 is fused to B-maggio and L27 is fused to mCherry. The fluorescence of B-maggio is green while mCherry is red (Shaner *et al.*, 2004). G. Time course of [100S]/[100S+70S] for S10-GFP (solid line), and S10-GFPΔ*yfiA* (broken line).

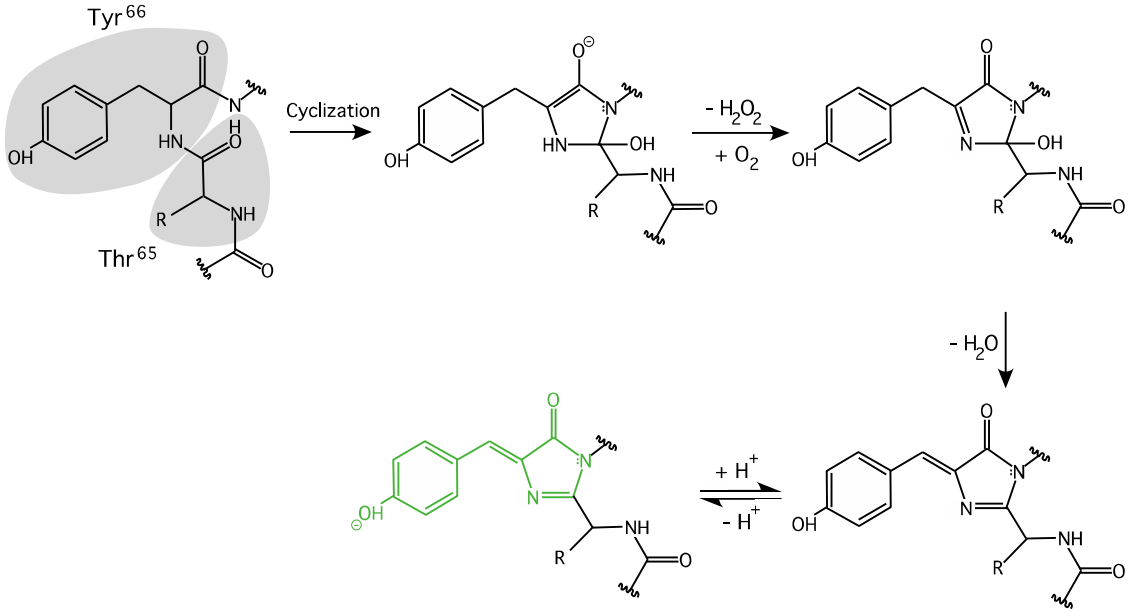

Figure 5. Maturation of the GFP fluorophore, 4-(p-Hydroxybenzylidene)-5-imidazolinone. (Adapted from Stepanenko et al., 2011).

Green chromophore synthesis comprises three stages: cyclization, oxidation to cyclic imine, and dehydration of Tyr66, which results in a mature GFP-like chromophore which is able to emit green light in a deprotonated (anionic) state. The fluorescent form of the chromophore is shown in green color. The residue at the position 65 is diverse among GFP-like proteins; in B-Maggio there is Threonine in this position.

Table II. List of property enhancing mutations in fluorescent proteins.

Name of fluorescent protein	Original protein	Changes introduced to the original protein
Venus	YFP	F46L/F64L/M153T/V163A/S175G
GFPuv4	GFP	F64L/S65T/F99S/M153T/V163A/S208L
B Maggio	GFP	C48S/F64L/S65T/Q80R/M153T/V163A/Q204C
mCherry	mRFP1	Q66M/V71/T147S/M163Q/M182K/T195V Additionally, 6 N-terminal residues were substituted for 11 N-terminal residues of GFP, and the last C-terminal residue was substituted for 7 C-terminal residues of GFP

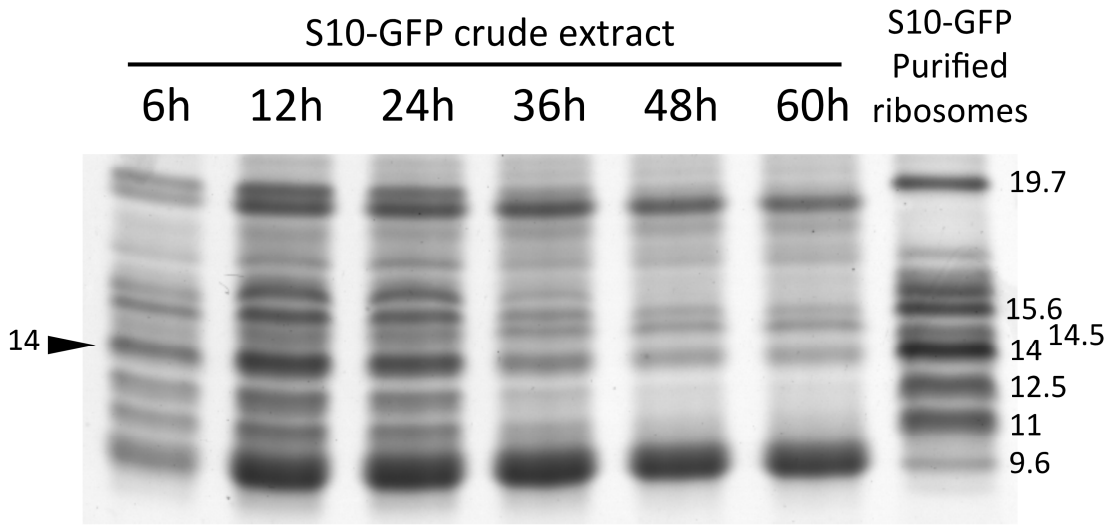

Figure 6. 14k band in 10-20k region of the SDS-polyacrylamide gel.

Electrophoretic pattern of proteins in the crude extract of the S10-GFP strain collected at different time points after inoculation is shown next to that of the purified S10-GFP ribosomes. Similar amounts of the crude extract (10% v/v of the crude extract, obtained from a fixed volume of liquid culture) were loaded for each time point.

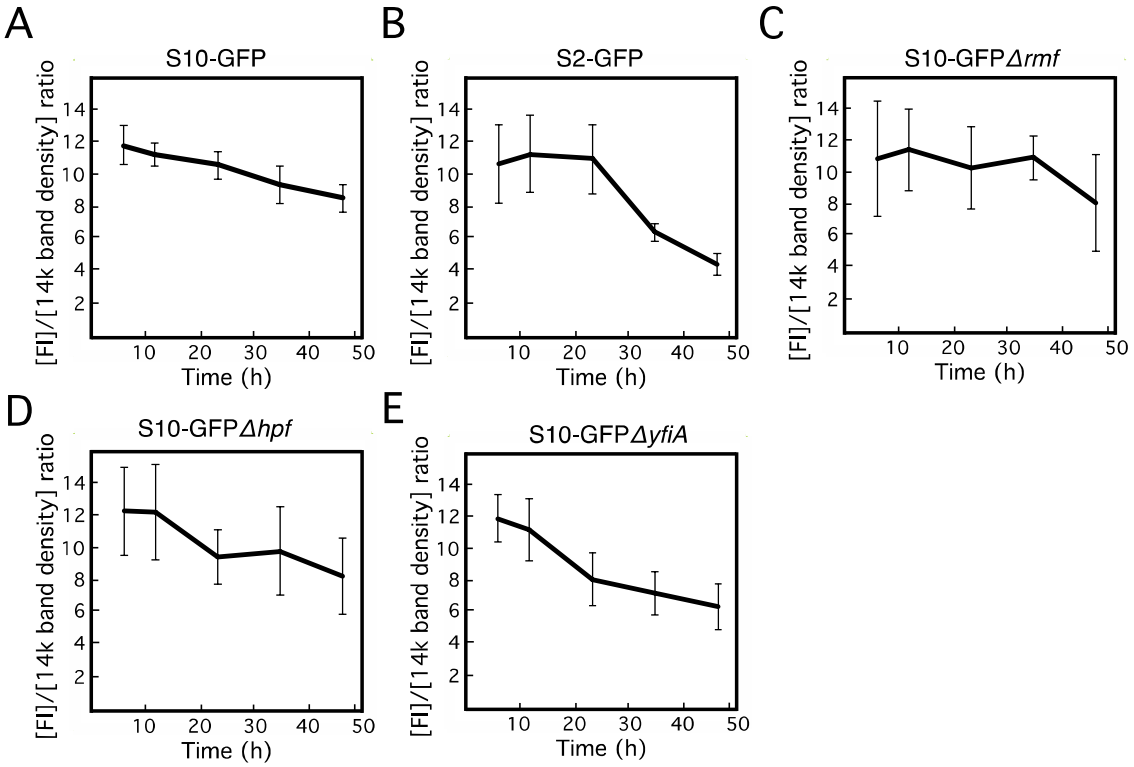

Figure 7. Time courses of ratios of fluorescence intensities of S10-GFP or S2-GFP protein to the densities of 14k band.

A-E. Ratios were calculated for every strain and each time point by dividing the intensity of the fluorescent band in SDS-polyacrylamide gel by the density of 14k band in the same Coumassie Brilliant Blue stained gel. The strains are indicated at the tops of the panels. Error bars represent SD (n=3—9).

Table III. Comparison of fluorescent intensities between different conditions

	Effect of/on	Comparison	Analyzed samples	Fluorescence intensity[α]	Protein (µg)[ε]	Ratio
1	gel media/ fluorescence	2% agarose[β]	cytosolic fraction of S10-GFP cells harvested at 12h	12.3±0.40		1.01 ± 0.05
		SDS polyacrylamide[γ]		12.2±0.42		
2	SDS/ fluorescence	no SDS	ibd.	12.8±0.29		1.07 ± 0.05
		0.5% SDS		12.0±0.59		
3	extracting temp./ fluorescence	room temperature	ibd.	12.5±0.78		0.97 ± 0.07
		37°C		12.8±0.29		
4	DTT/ staining 14k band[δ]	no DTT	aggregates fraction of S10-GFP cells harvested at 12h		0.67±0.07	1.0 ± 0.2
		10 mM DTT			0.65±0.09	

α: in arbitrary unit common to the numerator and the denominator

β: in 15 mM Mg2+, 100 mM NH4Cl, and 10 mM Tris HCl(pH 7.6)

γ: 12% polyacrylamide Wide-Range gel with Laemmli running buffer (containing 0.1% SDS)

δ: colloidal Coomasie Brilliant Blue staining calibrated with BSA

ε: For convenience in calculating the ratio, average and standard deviation are shown to the second decimal place

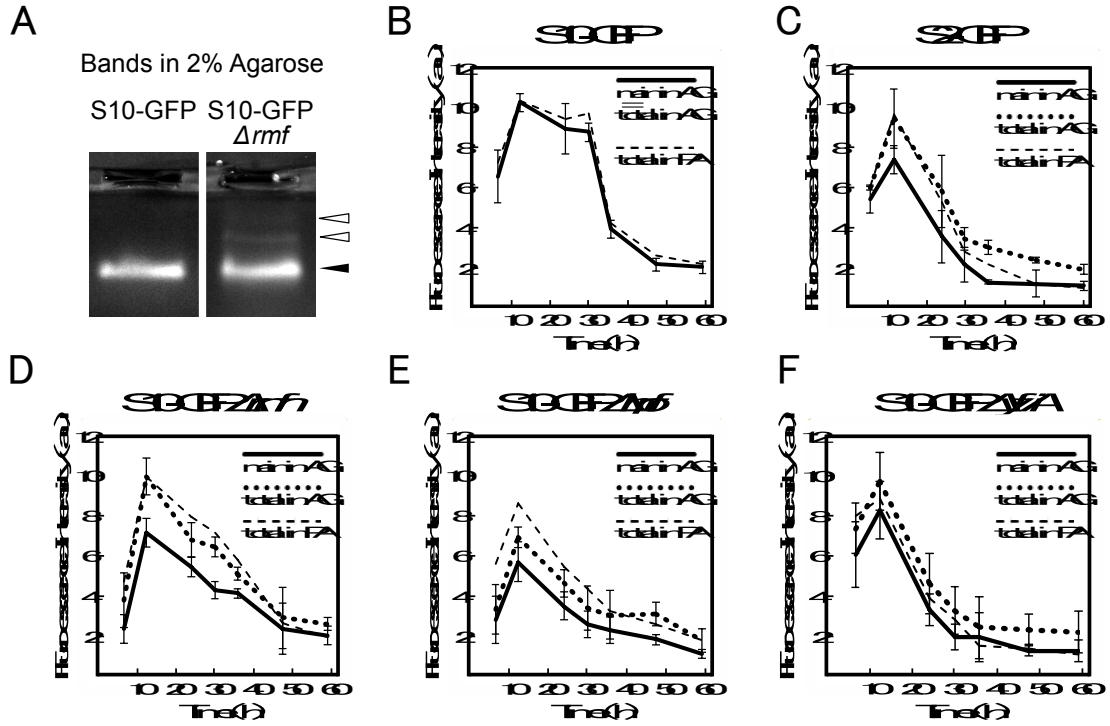

Figure 8. Fluorescence intensities of S10-GFP or S2-GFP proteins in cytoplasmic fraction analyzed by agarose gel electrophoresis or SDS-polyacrylamide gel.

A. Fluorescent images of the cytoplasmic fractions of S10-GFP (Left) and S10-GFPΔ*rmf* at 12 h in agarose gel. The filled arrowhead indicates the major fluorescent band, and the empty arrowheads indicate the minor fluorescence bands. B-F. The strains are indicated at the tops of the panels. The intensities of the major bands and the total intensities of bands (major + minor) in agarose gel (AG) are displayed by the line graphs as denoted in insets. Error bars represent SD (n=3—9). As a control, the band intensity in SDS-polyacrylamide gel (PA) is also displayed. Its standard deviations are omitted for simplicity in this figure but shown in Figure 9 as error bars. The scale of intensity is common for all the panels but is expressed in arbitrary units (au) specific to the fluorimeter.

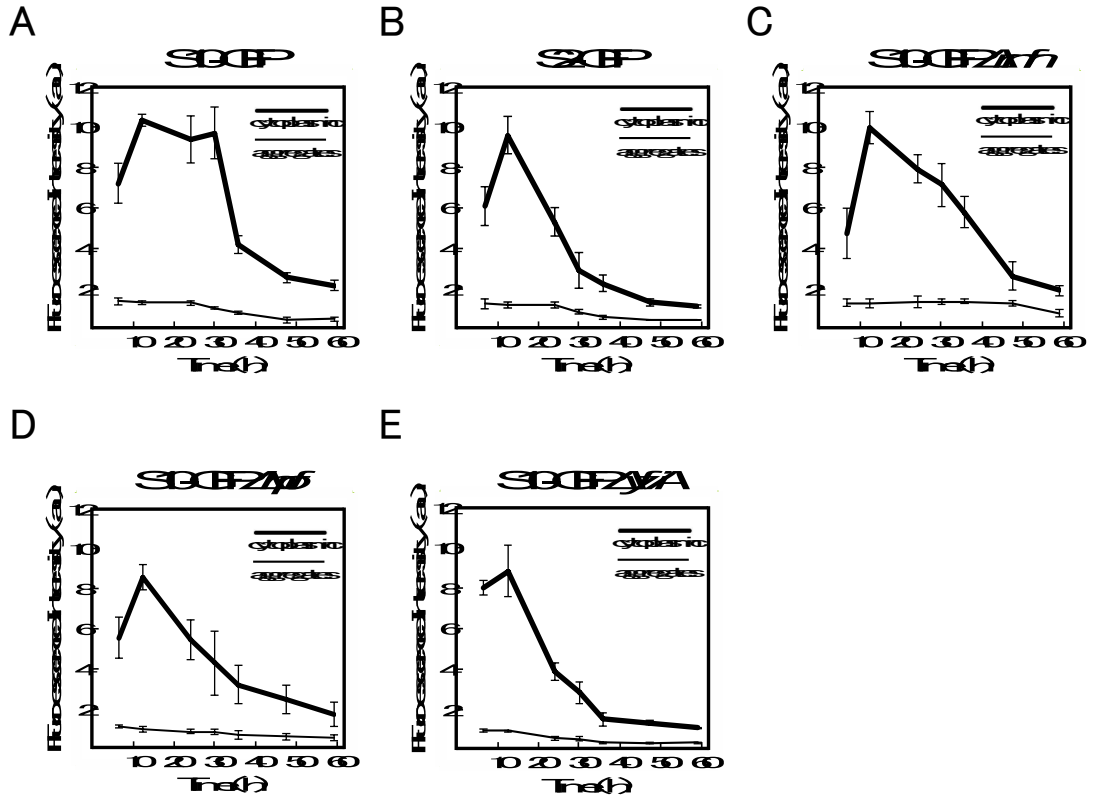

Figure 9. S10-GFP or S2-GFP protein in the cytosolic and the aggregate fractions.
The cytosolic and the solubilized aggregate fractions were analyzed by SDS polyacrylamide gel electrophoresis. The fluorescence intensities are displayed as line graphs as denoted in insets. The strains are indicated at the tops of the panels. The fluorescence intensities at each time points are plotted with errors obtained from 3-9 runs, and the strains are indicated at the tops of the panels. The scale of the intensity is common for all the panels in this figure as well as Figure 8, but expressed in arbitrary units (au). The cytosolic fraction is the combination of the first and the second extractions collecting 93%, and the latter is that of the first, the second, and the third extractions collecting 90%. The intensities for the latter are thus multiplied by 0.93/0.90 for comparison.

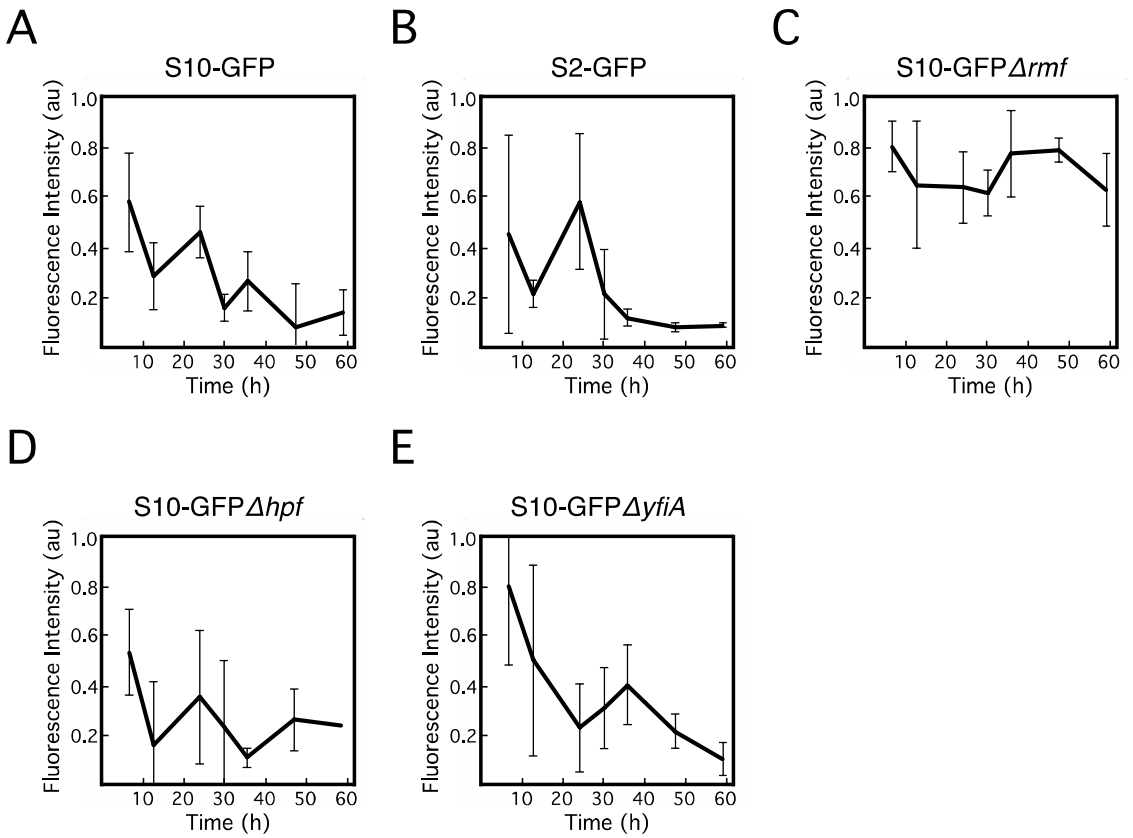

Figure 10. S10-GFP or S2-GFP protein in the aggregate fractions (corrected for contamination with proteins coming from the soluble fraction).

7% of the fluorescence intensities of the soluble fraction (thick lines in Fig.9) were subtracted from the corresponding intensities in the aggregate fraction (thin lines in Fig.9) and the obtained values were plotted against time for each strain. Names of the strains are indicated at the top of each panel. The scale of the intensity is common for all the panels in this figure as well as Figure 9, and is expressed in arbitrary units (au).

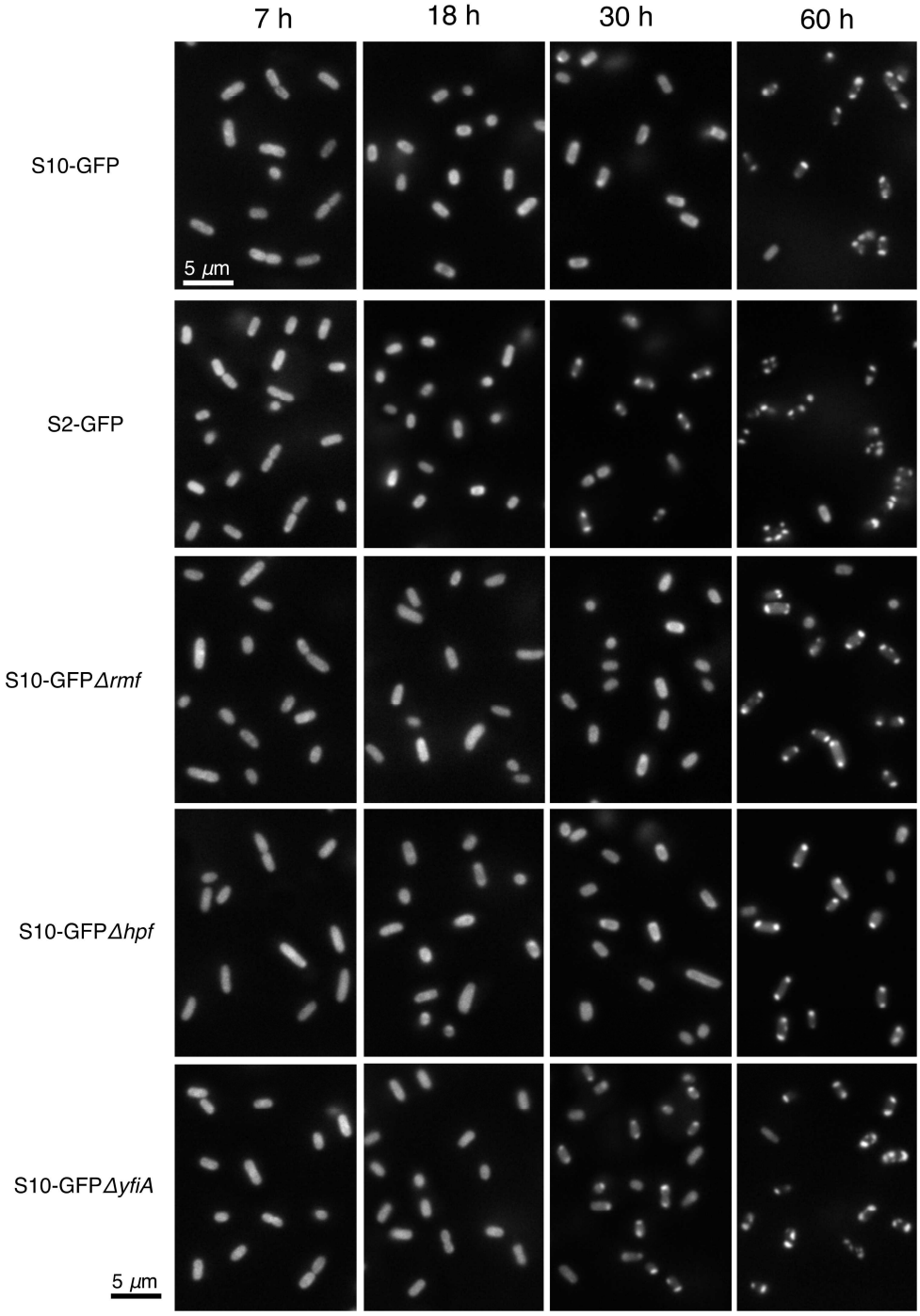

Figure 11. Microscopic observation of S10/S2-GFP fluorescence in single cells.
Names of the strains are indicated for each row of images on the left. Time at which the cells were examined is indicated at the top of the upper row of images. Note, that the contrast of the images was adjusted to optimally display the details of distribution of fluorescence. The fluorescence intensities cannot be compared among images presented in this figure.

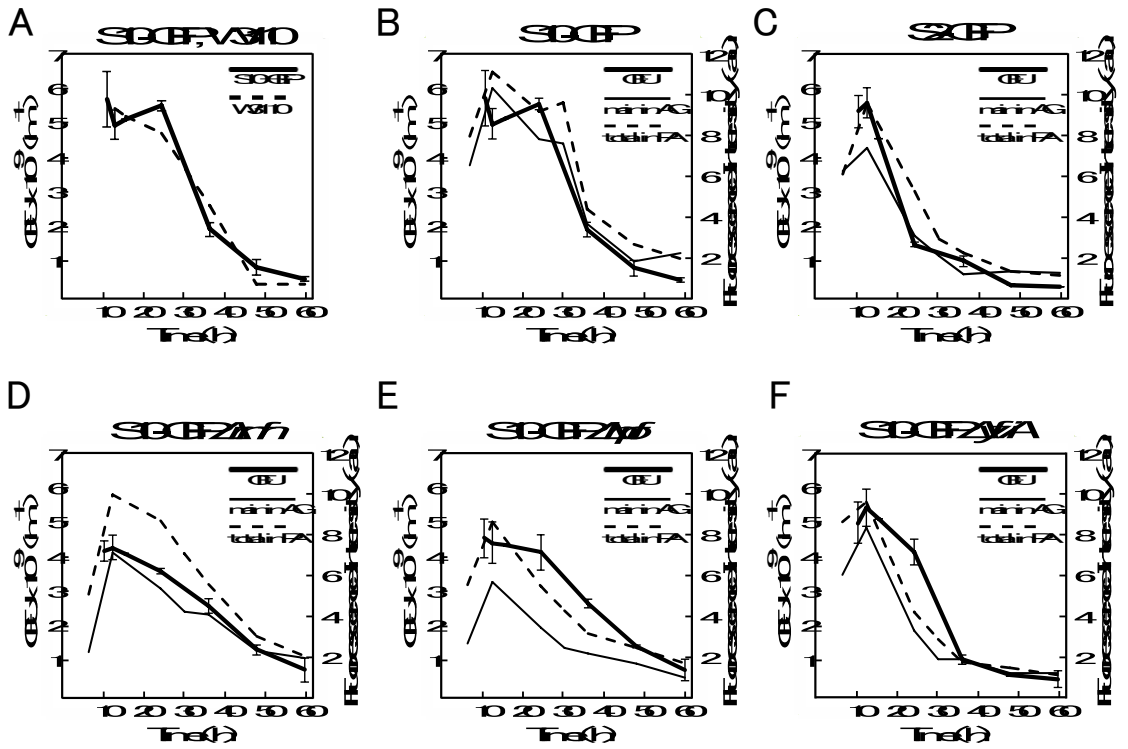

Figure 12. Time courses of CFU and their similarity to the fluorescence intensities of ribosomal bands.

A. The time courses of S10-GFP and W3110. B-F. The time courses of CFU as well as the time courses of the fluorescence intensities of the main bands in cytoplasmic fraction in agarose gels (AG) and the fluorescence intensities of the bands in SDS polyacrylamide gels (PA). The scale of the fluorescence intensities is the same as in Figures 8 and 9.

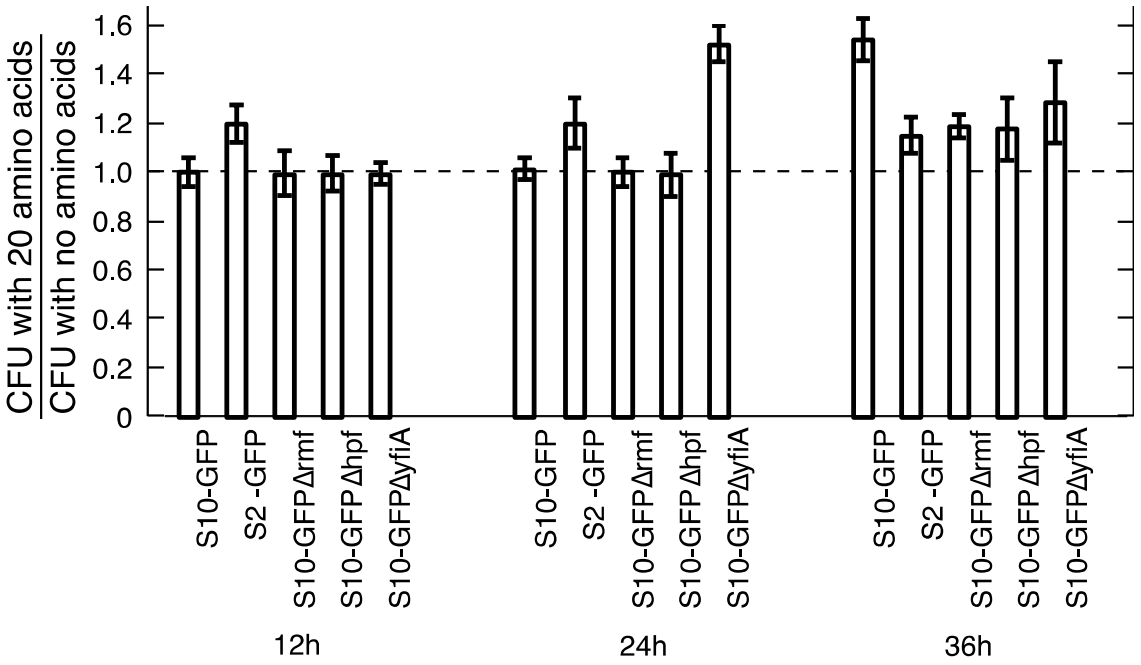

Figure 13. Effect of addition of 20 amino acids on CFU.

A solution of 12 mg each of arginine, cysteine, and tyrosine, and 60 mg of the other 17 amino acids was neutralized with NaOH and lyophilized in a 2 ml sample tube. A culture of 0.15 ml was added at the indicated time points and further cultured for 12 h. Bars represent means ± SD (n=5). See the text for more details.

Example of Possible Model	100S	Strain	12 h		24 h		36 h		Decay of ribosome and CFU
			aa pool size/ regeneration	degradation	aa pool size/ regeneration	degradation	aa pool size/ regeneration	degradation	
A	(a) More resistent to degradation than 70S	S10-GFP	+ / +	= + (a)	++ / ++	= ++	± / ±	++	plateau and then rapid
		S10-GFPΔrmf	++ / ++	= ++	+ / +	++	± / ±	+	slow
		S10-GFPΔhpf							
		S2-GFP	± / ± (2)	= ± (2)	± / ± (2)	+ (2)	± / ± (2)	++	rapid
		S10-GFPΔyfiA	+ / +	= + (a)	± / ±	+ (1)	± / ±	++	rapid
B	(b) More suceptible to degradation than 70S	S10-GFP	+++ / +++	= +++ (b)	++ / ++	= ++	± / ±	++	plateau and then rapid
		S10-GFPΔrmf	++ / ++	= ++	+ / +	++	± / ±	+	slow
		S10-GFPΔhpf							
		S2-GFP	± / ± (2)	= ± (2)	± / ± (2)	+ (2)	± / ± (2)	++	rapid
		S10-GFPΔyfiA	+++ / +++	= +++ (b)	± / ±	+ (1)	± / ±	++	rapid

Common hypothesis

(1) YfiA-free 70S is more resistant.

(2) S2-GFP makes aa pool size smaller and degradation starts later than S10-GFP.

Figure 14. Two possible models of 100S role in protein turnover.

For detailed information see the text. Red and blue colors indicate the differences in interpretation of the obtained results depending on the proposed model.

Table IV. *E.coli* strains, used in this study.

Strain name	Modifications introduced to W3110
HN 3611	*rpsJ-gfp*
HN 3561	*rpsB-gfp*
HN 3615	*rpsJ-gfp, Δrmf*
HN 3616	*rpsJ-gfp, Δhpf*
HN 3023	*rpsJ-gfp, ΔYfiA*
HN 3780	*rpmA-gfp*

Table V. Yields of the extractions of soluble fraction and aggregate fraction.

Extraction of soluble fraction

extract [α]	e1	w1	w2	w3
cummulative yeid of extraction (%)	69±5	93±0	99±1	100

Extraction of aggregate fraction

extract [α]	e1	e2	e3	e4	e5	e6	e7
cummulative yeid of extraction (%)	52	76	84	92	96	99	100

[α]: "e" stands for extraction for 5 mins in the appropriate buffer with shaking, "w" stands for washing the pellet with an appropriate buffer
In the routine experiments, for the soluble fraction, e1 and w1 were combined, and w2 and w3 steps were omitted. For the aggregate fraction, e1, e2 and e3 were combined, and the following extraction steps were omitted.

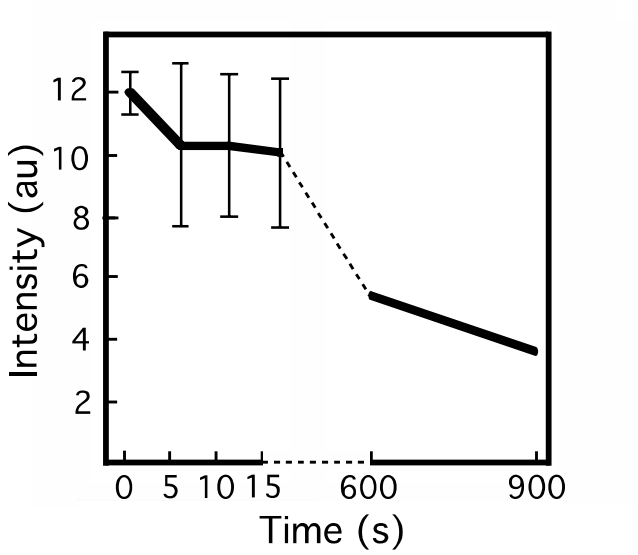

Figure 15. Decrease of the intensity of the LED lamp light.

A blank white sheet of paper was irradiated with a LED lamp and a photo of the sheet was taken immediately after switching the lamp ON and after various time intervals. The intensity of the excitation light was measured with ImageJ (NIH, Bethesda) as the mean integrated density of the sheet (displayed in arbitrary units specific for this figure), and plotted against time.

Table VI. Intensity of the excitation light in the area of fluorescence measurements.

86	87	89	90	91	92	94	94	95	96	97	98	98	98	99	99	99	99	98	97
86	87	89	90	92	93	94	95	97	98	99	99	99	99	99	98	98	99	98	97
85	86	88	89	91	92	94	95	97	98	100	100	100	99	99	99	99	99	98	98
84	85	86	88	89	91	92	94	96	97	99	99	100	99	99	99	99	99	99	98
83	84	85	87	88	90	91	92	94	95	97	98	98	98	98	98	98	99	99	99
84	84	85	87	88	90	91	92	93	93	95	96	96	97	97	97	97	98	98	98

The area of the surface, where the gels were placed for fluorescence measurements was divided into 6 x 20 regions. Intensity of the excitation light was measured in each region with ImageJ (NIH, Bethesda) as the optical density of the region in the photo of a blank white sheet. The intensity is displayed as % of the maximum intensity.

Table VII. Settings of the GRADIENT MATE 6T machine used to prepare the 5%—20% sucrose gradient.

roter	cap	solution	top	bottom	unit	step	time	angle	speed
Sw40	short	SUCR	5	20	w/v	1	1:55	81.5	15

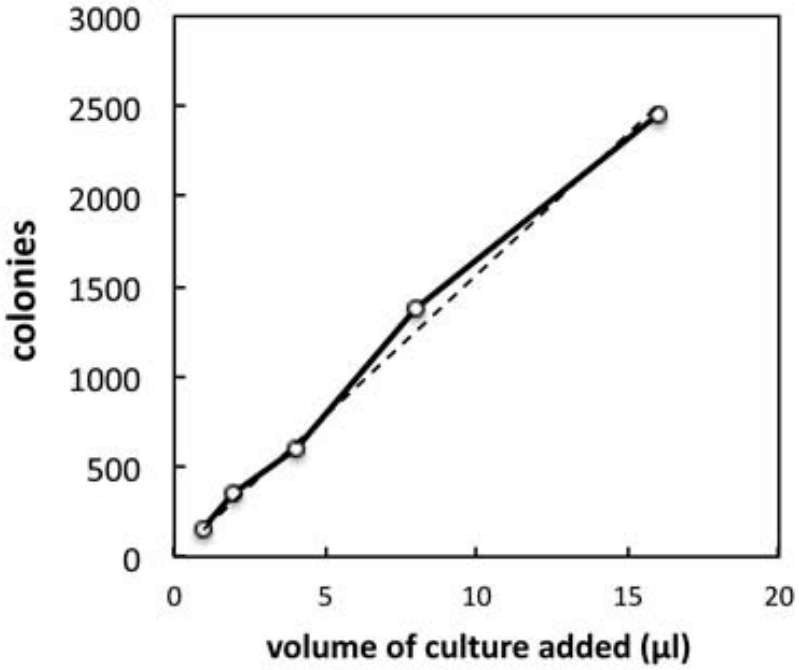

Figure 16. The linearity of CFU counting.

Various volumes of a 1000-fold diluted LB culture of W3110 were added to the plate, and colonies were counted on LB plates (open circles). The broken line shows the least-square fitted line with zero intersections. Linearity was observed at least up to 2500 colonies.